Title: The properties of individual fire events are essential for understanding global fire regimes

Authors: Adam L. Mahood[1,2], Ty Tuff[1,3], Megan E. Cattau[4], Virginia Iglesias[1,3], Thomas E. Hanson[5], Jilmarie Stephens[1,6], Nayani Ilangakoon[1], Maxwell C. Cook[1,7], R. Chelsea Nagy[1,3], David Barnard[2,8], E. Natasha Stavros[1,9], Amy DeCastro[1,7,10], Jennifer K. Balch[1,3,7]

Affiliations:
1. Earth Lab, CIRES, University of Colorado Boulder
2. Water Resources Systems Management, USDA-ARS
3. Environmental Data Science Innovation and Inclusion Lab, CIRES, University of Colorado Boulder
4. Human-Environment Systems, Boise State University
5. Anthropology, University of Colorado Boulder
6. North Central Climate Adaptation Science Center, Boulder, CO
7. Geography, University of Colorado Boulder
8. Ecosystem Science and Sustainability, Colorado State University
9. WKID Solutions LLC
10. National Center for Atmospheric Research

Corresponding Author: admahood@duck.com

ORCID IDs, emails:
Mahood: 0000-0003-3791-9654 admahood@duck.com
Tuff: 0000-0001-5249-5197 ty.tuff@colorado.edu
Cook: 0000-0003-4865-5025 maxwell.cook@colorado.edu
Stavros: 0000-0001-6657-7310 enstavros@gmail.com
DeCastro: 0000-0002-7496-6516 dramydecastro@gmail.com
Nagy: 0000-0002-7168-3289 chelsea.nagy@colorado.edu
Cattau: 0000-0003-2164-3809 megancattau@boisestate.edu
Barnard: 0000-0003-1877-3151 david.barnard@usda.gov
Iglesias: 0000-0001-5732-3714 virginia.iglesias@colorado.edu
Stephens: 0000-0002-0066-2974 jlimarie.stephens@colorado.edu
Balch: 0000-0002-3983-7970 jennifer.balch@colorado.edu
Hanson: 0009-0008-9816-5458 thomas.hanson@colorado.edu

Keywords: Wildfire, fire events, fire growth rate, burned area, vapor pressure deficit

Data and Code Availability: All data and code are freely available at https://github.com/admahood/global-fire-regime-trends (Mahood and Cook, 2025)**.**

Author Contributions: Conceptualization: ALM, TT, MCC, ENS, JKB; data curation: ALM, MCC; formal analysis: ALM, TT, TEH, JS, MCC, NI, MEC; funding acquisition: JKB, RCN; Investigation: ALM, TT, MEC, TEH, JS, NI; methodology: ALM; MCC; VI; project administration: ALM, JKB; supervision: JKB, DB; visualization: ALM; writing - original draft: ALM, MEC, TEH, JS, MCC, NI; writing - review & editing: ALM, TT, RCN, MEC, TEH, VI, JS, MCC, NI, ENS, DB

Abstract

Aim: As fire activity changes globally, we need to better understand the spatial and temporal characteristics of the individual events that, when aggregated, constitute fire regimes. Most global studies analyze point detections of burned area, without delineating or considering the properties of individual events. Furthermore, there is a critical need to understand fire patterns within the context of the geopolitical boundaries within which fires are managed.

Location: Global

Time period: 2003-2020

Major taxa studied: Fire

Methods: We divided 241 countries by Köppen-Geiger climate classifications and quantified four event-based fire regime metrics: size, duration, and mean and maximum growth rate; and four area-based metrics: burned area, number of fires, season length, and season peak. We examined the correlations among fire regime components, and between each fire regime component and climate normals. We quantified temporal trends, and used mixed models to analyze how climate and landcover change were associated with event-based components of fire regimes.

Results: Event-based metrics were weakly correlated with area-based metrics. Countries with warmer and less variable climates had high burned area, more fire events, longer season lengths and shorter event durations. Countries with high annual temperature range and low precipitation tended to have fewer events but larger fires that were faster-spreading and occurred later in the year. The growth rate and size of individual fire events are increasing in 18% and 21% of regions we analyzed, respectively. Interannual variability in size and growth rate were associated with aridity increases in boreal areas, and landcover changes in arid areas.

Main Conclusions: Drivers of burned area and fire seasonality are well-understood but largely unrelated to the properties of individual events. A more detailed understanding of the spatial and temporal aspects of fire events at broad scales will assist fire management efforts in preparing for a warmer future.

Introduction

As fire activity changes across the globe, we need to better understand the spatial and temporal characteristics of the individual fire events that, when aggregated, constitute important components of regional fire regimes. Fire regimes have many facets, some of which can be understood by aggregating burned pixels or events across an area, and do not require information about how individual events unfold. These area-based metrics include season length, season peak, burned area and number of events. Much of the current understanding of global fire regimes centers around these aspects of fire regimes. Globally, burned area has declined since 2000 (Andela *et al.*, 2017; Chen *et al.*, 2023) despite global increases in aridity, temperature and fire season length (Jolly *et al.*, 2015). By the end of the century, however, changes in climate are expected to drive global increases in burned area (Moritz *et al.*, 2012), and in many areas around the world such expectations are now becoming fulfilled. For example, increasing temperatures and aridity have been linked to observed increases in area burned in the western United States (Dennison *et al.*, 2014; Abatzoglou and Williams, 2016) and in boreal forests (McCarty, Smith and Turetsky, 2020; Whitman *et al.*, 2022; Grünig, Seidl and Senf, 2023).

Other facets of fire regimes require understanding the properties of individual events. These event-based metrics include size, growth rate, severity, intensity, duration, and event complexity (White and Jentsch, 2001; Sugihara, Van Wagtendonk and Fites-Kaufman, 2006). The properties of individual fire events are as important as regionally aggregated metrics for understanding fire regimes (Pais *et al.*, 2023). Event-based metrics allow us to better understand situations like that in Northern Europe, for example, where burnable land is decreasing due to changes in land use, but the remaining flammable areas are experiencing larger and more intense fires due to aridity increases (Grünig, Seidl and Senf, 2023). The properties of individual fire events, and how they are driven by social and environmental factors at broad scales, are crucial for reducing socioeconomic damage (Iglesias, Balch and Travis, 2022). The speed at which an individual fire spreads is primed by long-term trends in aridity (Luo *et al.*, 2024), but driven day to day by fine scale weather. Of course, the more a fire spreads the larger it inevitably becomes, and fires that spread faster are more likely to become larger (Coop *et al.*, 2022). Larger, faster-spreading fires have a higher chance of causing human casualties and destroying structures (Higuera *et al.*, 2023) as well as having greater impacts on ecosystems (Jones *et al.*, 2021; Hantson *et al.*, 2022). Events of extreme intensity and spread rate are already becoming more common and are expected to increase with future warming (Balch *et al.*, 2022; Coop *et al.*, 2022; Cunningham, Williamson and Bowman, 2024).

One of the reasons that events have received less attention at broad scales is that there is limited data on event boundaries at those scales. Delineating event boundaries at broad scales from gridded data for thousands if not millions of events requires significant and costly computing resources, expertise and attention to detail. One must define a spatio-temporal window in which to aggregate pixels or point detections together into events, and the optimum window size varies from place to place (Cattau *et al.*, 2016; Andela *et al.*, 2018; Balch *et al.*, 2020; Coop *et al.*, 2022; Mahood *et al.*, 2022). Some countries produce data products on individual fire events (Eidenshink *et al.*, 2007; Barber *et al.*, 2024), but this is rare outside of the most affluent countries. Many studies also claim to be analyzing events, but consider all individual point detections (typically representing 0.25 - 2 km^2, depending on the product) as ‘events’. Therefore most English-language published global analyses examine trends and patterns in unaggregated, satellite-derived point detections of burned area or hotspots (Archibald *et al.*, 2013; Andela *et al.*, 2017; García *et al.*, 2022) (but see (Balch *et al.*, 2022)).

Fire regimes are becoming increasingly recognized by western scientists as a social-ecological phenomenon (Balch *et al.*, 2016; Taylor *et al.*, 2016; Higuera *et al.*, 2023). Humans influence fire regimes via climate change (Abatzoglou and Williams, 2016), fire suppression, the introduction of ignitions (Balch *et al.*, 2017; Cattau *et al.*, 2020), by affecting fuels through land use (Giglio, Randerson and Van Der Werf, 2013; Andela *et al.*, 2017; Earl and Simmonds, 2018; Ward *et al.*, 2018; García *et al.*, 2022) and the introduction and spread of invasive plants. These fuel alterations can either increase (Fusco *et al.*, 2019, 2021) or decrease (Collins *et al.*, 2021) fire activity depending upon their effect on flammability, fuel load, and fuel continuity (Keeley and Pausas, 2019; Mahood, Koontz and Balch, 2023). National policies often govern fire suppression efforts. For this reason, in order to understand how geopolitical factors affect fire activity and the social-economic-environmental burden that fire imposes on different countries, it is essential to consider the boundaries within which policies are implemented and where fires occur.

Here, we describe recent global patterns and trends in fire regime properties as delineated by national boundaries and coarse Köppen-Geiger (KG) climate regions (**Fig. 1**). We used a collection of country-level fire perimeter datasets (Mahood *et al.*, 2022) for 241 countries from 2003-2020 to examine four event-based attributes: size, duration, mean daily growth and maximum daily growth, as well as four area-based attributes: burned area, number of fires, season length, and season peak (day of the peak in burned area). We had three objectives. First, we examined spatial patterns for all 241 countries, and temporal trends in 145 countries with consistent fire activity. Second, we explored the correlations among the fire regime attributes, and among fire regime attributes and climate normals. Third, because event-based attributes of fire regimes are relatively understudied, we explored whether annual trends in event-based attributes followed expectations of fuel versus energy limitation (Kelley *et al.*, 2019). We hypothesized that in boreal regions, aridity increases would be associated with increased fire activity due to their abundant fuel, low temperatures, and high fuel moisture. In arid regions, we hypothesized that instead of aridity increases, changes in landcover, which are driven by human activity, would be associated with interannual variation in fire regimes. We illustrate this through examples where the authors happen to have situated knowledge gained via direct experience (Bennett *et al.*, 2022).

Methods

Fire Data

We used a collection of fire perimeter products derived for each country that had appreciable burned area (Table S1 from (Mahood *et al.*, 2022)). These products were created using the FIREDpy algorithm (Balch *et al.*, 2020) aggregates burn date pixels from the MODIS MCD64 burned area product (Giglio *et al.*, 2018) into events using a spatiotemporal moving window. The fire perimeters used here had a temporal extent from November 2001 to between March and May of 2021. Because the Terra and Aqua satellites which bear the MODIS sensors were not launched at the same time, and because the datasets had only a portion of 2021, we truncated the data to 2003-2020 for temporal comparisons and annual trend estimates 2003 to 2020.

Event-based attributes*:* We derived four fire regime attributes for each KG climate zone within each country that were based on the properties of individual fire events: fire event size (ha), fire duration (days), mean fire growth rate (ha/day), calculated as burned area divided by duration, and maximum single day growth (ha), which was the area burned on the day with the most area burned.

Area-based attributes: We also derived four fire regime attributes for each KG climate zone within each country that were based on aggregating events to a broad area. We used the ignition date calculated for each event to derive fire season length (days). This was the standard deviation of ignition day of year weighted by burned area. Fire season peak (day of year) was calculated as the mean of ignition day of year across all events weighted by burned area. The number of events was calculated as the count of fires divided by the area of the region. Finally, total burned area (km^2) was calculated as the area burned divided by the total area of the region. Both area-based and event-based metrics were calculated for the entire time period (2000-2020) to examine spatial patterns, and at annual timesteps in order to analyze temporal trends. We also calculated each attribute, and trends in each attribute, for each country. Maps and tables of these are given in the supplement (**Tables S2-S6, Fig. S1**).

Climate Classification: After being delineated by country, we assigned each fire event to the coarse KG climate region (Equatorial, Arid, Temperate, Boreal, or Polar) that encompassed a plurality of fire's area (Beck *et al.*, 2018). We used coarse KG climate regions because they align well with broader fire regimes, and they have been used in other fire regime studies (Balch *et al.*, 2022; Zhang *et al.*, 2025). For example, Cattau et al (2022) found that US fire regimes broadly had an east to west divide, with secondary divides in the west determined by elevation, and in the east determined by latitude. This is readily apparent in **Fig. 1a**. The U.S. is also an outlier in this regard—most countries fall into generally the same coarse KG category (**Fig. 1b**). All trends and patterns were calculated with the combination of country and KG climate region as the base unit of analysis. Polar regions were excluded due to small sample sizes.

Ancillary Data

In order to understand how spatial patterns in fire regimes were correlated with climate normals, we calculated the median of 19 WorldClim bioclimatic variables for each KG climate region within each country (Fick and Hijmans, 2017). In order to examine the effects of land-cover change on fire regimes, we extracted the annual area (km^2) of cover types for each KG climate region within each country from the 500 m resolution MODIS MOD12Q1 V6 (Sulla-Menashe and Friedl, 2018) using the Annual International Geosphere-Biosphere Programme (IGBP) classification scheme. We aggregated the IGBP classification into four general categories; cropland, grassland, forest, and urban/built-up.

Vapor pressure deficit (VPD) is the difference between the amount of moisture in the air and the maximum amount of moisture the air can hold at its current temperature (Anderson, 1936; Seager *et al.*, 2015). It is strongly associated with fire activity (Sedano and Randerson, 2014; Williams *et al.*, 2014), plant water stress (Yuan *et al.*, 2019; Grossiord *et al.*, 2020) and fuel moisture (Resco De Dios *et al.*, 2022; Griebel *et al.*, 2023). Within the burnable land area for each KG climate region with each country, we extracted the mean VPD during the fire season months for each country from TerraClimate, a 4-km gridded data set of global monthly climate variables (Abatzoglou *et al.*, 2018). Fire season months were defined using the peak season day and the season length information derived from FIRED (see Section **2.1**). We calculated the fire season VPD anomaly by subtracting the annual mean from the long-term mean (1958-2022) during the same months.

Statistical Analysis

We used Pearson's product moment correlation coefficient (Stigler, 1989) to test for association between each pair of fire regime attributes, and for each attribute against bioclimatic variables from WorldClim (Fick and Hijmans, 2017). We used an alpha value of 0.05 to assess significance.

We used median-based linear regression models with repeated medians (Siegel, 1982) to calculate the temporal trend in each fire characteristic for each KG region within each country with more than 20 fires in both the first nine years and the second nine years of the time period (n=268). We used alpha = 0.05 to determine significance.

To explore the drivers of interannual variability in event-based fire regime components, we created linear mixed models (Bates *et al.*, 2015) for each fire regime component for arid and boreal KG climate regions within countries that had at least one fire event in 15 of the 18 years analyzed. We created one model for each component for the arid regions (n=70) and another set of models for the boreal regions (n=43). Annual estimates of land cover (forest, grassland, cropland, and urban/built up) and mean VPD were predictors. Because landcover changes are associated with human activity, we included Country and World Bank Subregion (Kelso and Patterson, 2010) as random effects. All response variables except season length and season peak were log-transformed.

Results

Spatial patterns in fire regime attributes

For area-based fire regime attributes, there was higher burned area, more fire events, and longer season lengths at low latitudes (**Fig. 2a**). Event-based attributes had a different pattern. The countries with the largest and fastest spreading fires were mostly at middle latitudes, while countries with the longest lasting fires were mostly in Central and South America, Saharan Africa and the Eurasian Steppe (**Fig. 2b**).

Correlations among fire regime components and climate normals

Event-based fire regime attributes tended to be weakly correlated or unrelated to area-based fire regime attributes, and were correlated with different climatic normals. Burned area and number of fires (both were adjusted for the area of the country) were strongly correlated (Pearson's $r = 0.84$, **Fig. 3a**). Number of fires was negatively related to event duration ($r = -0.32$). Burned area ($r = 0.25$) and number of fires ($r = 0.2$) were also positively correlated with fire season length. These three characteristics had positive associations with warmer temperatures and lower annual temperature range, as well as high precipitation seasonality (**Fig. 3a**). Burned area and season length were unrelated to fire event size and growth rate. Rather, fire size was associated with maximum single day growth ($r = 0.65$) and mean fire growth rate ($r = 0.5$). Number of fires was unrelated to fire size, and negatively correlated to mean and maximum growth rate ($r = -0.12$, -0.12, respectively). Areas with faster growing fires tended to have fewer fires ($r = -0.12$). High fire size and mean and maximum growth rates were associated with high annual and diurnal temperature ranges, and with lower mean annual temperatures and temperatures of the coldest months (**Fig. 3b**). Maximum single day growth had stronger correlations with other fire regime attributes and with climate variables than mean growth rate in all cases analyzed here. Maps and tables of all eight fire regime components delineated by country are in **Fig. S1** and **Tables S2-S6).**

Temporal Trends

Trends in burned area and number of fires followed similar spatial patterns (**Fig. 4**), and had mostly negative (118 and 104 regions) and neutral trends (**Table 1, Fig. 4**). In contrast, season length and season peak had more positive (71 and 56) than negative (43 and 45) trends. Size, Mean fire growth rate and maximum single day growth also followed similar spatial patterns (**Fig. 4**), with many positive trends across the tropical Americas and Oceania, but still with more negative trends (83, 90 and 89) than positive (56, 49 and 47). Event duration had different spatial patterns than the other event-based characteristics, 49 regions had positive trends and 56 had negative trends (**Table 1, Fig. 4**).

Associations between annual estimates of fire regime components, climate and land cover

For the models of fire size, mean growth rate and maximum growth rate, fixed effects (annual estimates of forest, grassland, cropland, and urban/built up cover, mean VPD, and the interaction of all variables with the modal KG climate region) from linear mixed models explained 4%-21% of the variation. The random effects of World Bank subregion and country explained 38-67% of the variation **(Table S7).** For duration, the fixed effects explained 1% or less of the variation, and none of the fixed effects were significant. Cropland cover was not significant in any models. In arid regions, Increases in VPD were not associated with changes in any fire regime component. Rather, increases in urban and forest cover were associated with decreased size and growth rate, while increases in grassland cover were associated with increased size and growth rate **(Fig. 5)**. In boreal regions, increases in VPD were associated with increases in size, mean growth rate and maximum growth rate **(Fig. 5).**

Discussion

Our results showed that event-based attributes were strongly correlated with each other and weakly correlated at best with area-based attributes (**Fig. 3a**). They were also associated with different climatic variables than area-based attributes (**Fig. 2-3**), and the interannual variability in event-based attributes followed expectations of fuel versus energy limitation. Many countries with negative or neutral trends in burned area were also seeing positive trends in size and growth rate (**Figure 4**). Therefore, conclusions about fire activity based on analyses of burned area alone may be misaligned with those based on event-based attributes.

Relationships between event- and area-based fire regime attributes may be important for understanding and predicting different aspects of fire regimes. That burned area was weakly correlated to size and not correlated with growth rate is notable (**Fig. 3a, Fig. S2**). It suggests that in the world's most fire-prone places (e.g. Sub-Saharan Africa, Australia; **Table S1**), large values of annual burned area are more a function of the accumulation of small events rather than individual events consistently becoming large. The size of a particular event is controlled by the day-to-day spread rate, as evidenced by the strong relationship between event size and maximum single day growth ($r = 0.651$), which is more circumstantial and dependent on short-term weather (Coop *et al.*, 2022; Hantson *et al.*, 2022) than climatic norms (Balik *et al.*, 2024). These more circumstantial fire attributes are more difficult to model at coarse spatial and temporal scales (Brown *et al.*, 2023), but they may be more important for policy makers than burned area since the speed of the fire is more likely to cause problems with response and safety (Coop *et al.*, 2022; Hantson *et al.*, 2022; Balch *et al.*, 2024).

Humans have always coexisted with fire (Bowman 2009), and associations among fire regime components, as well as between fire regime components and aspects of climate, may be reflective of the socioecological nature of global fire regimes. Intentionally ignited fires tend to be small (<10 ha) (Kasoar *et al.*, 2024), and fire regimes with larger fires have been shown to be negatively correlated with human development (Archibald *et al.*, 2013). In areas with long growing seasons, fires may be more likely to be small, human-ignited and used for the management of croplands and pastures (Cattau *et al.*, 2022). In areas with short growing seasons, fire activity may be more circumstantial and dependent on factors such as topographic complexity, wet-dry oscillations, and extreme climatic events that drive extreme fire events mostly outside of human control. In the coterminous US, for example, smaller, more frequent, and human-caused fires occur in the southeast almost year-round, while larger, faster-spreading fires occur in the west, mainly during the summer (Cattau *et al.*, 2022).

The many neutral relationships we observed were expected given the short extent of the time series and the multifaceted nature of fire. A case study of two countries with similar climates, namely Sri Lanka and Indonesia, illustrates complexities that underlie the mixed trends. Sri Lanka has a clear country-wide decline in burned area that is strongly correlated with increases in urban land area (Pearson's r = -0.84, $p << 0.01$). However, in the remaining grasslands and forested areas on the north and east side of the island, increases in VPD are associated with fires that are larger, spreading faster, and lasting longer (Heenatigala, 2021). These dynamics contrast with those documented in previous studies in Indonesia or Southeast Asia more generally indicating no trends in overall fire activity (Andela *et al.*, 2017; Earl and Simmonds, 2018; Vadrevu *et al.*, 2019; Vetrita and Cochrane, 2019; Sloan *et al.*, 2022). In agreement with these studies, we found no statistically-significant trends in area burned or number of fires in Indonesia. However, we did find trends in event-based attributes: an individual event in 2020 was on average 10.8 ha larger ($p << 0.01$) and spread 5.4 ha/day faster ($p << 0.01$) than in 2003. These trends were most strongly associated with VPD increases (Pearson's $r = 0.74$, 0.84, respectively, both $p << 0.01$) as well as increases in urban land cover (Pearson's $r = 0.83$, 0.65, respectively, both $p << 0.01$).

Annual changes in event-based fire regime attributes are consistent with fuel versus energy limitations

Trends in the number of fires and burned area observed here agree with other studies that have shown a global decline in burned area driven by trends in urbanization and agricultural intensification in equatorial grasslands and savannas (Andela *et al.*, 2017; García *et al.*, 2022). Associations between event-based fire regime components and changes in annual land cover and VPD estimates followed expectations of fuel versus energy limitation (Krawchuk and Moritz, 2011; Kelley *et al.*, 2019; Novick *et al.*, 2024). That is, we expected that aridity increases would exacerbate fire activity in wet, productive places where, in general, fuel is plentiful but fuel moisture is high. Conversely, in arid countries, we expected that increases in atmospheric aridity would inhibit vegetation growth (Yuan *et al.*, 2019) and so fire activity would not increase in response to increased VPD, and that is what we found (**Fig. 5**). Changes in VPD had neutral relationships with all fire regime components in arid countries, and instead land changes were the main drivers. In these countries, increases in grassland cover were associated with higher burned area, more fire events, larger fire events and higher maximum single day growth. Increases in urban/built cover were positively associated with higher mean and maximum growth, and increases in forest cover and cropland were associated with smaller and slower-spreading fires.

In boreal countries six of eight fire regime components (burned area, number of fires, fire size, duration, mean and maximum growth) were positively associated with increases in VPD **(Fig. 5**). This was expected because high fuel loads associated with wet, historically infrequently burned forests that are energy-limited are being exposed to comparatively larger aridity increases than the rest of the world due to arctic amplification (Serreze and Barry, 2011). These regions may be approaching a situation where they are increasingly likely to have years where their energy-limitation is weakened during the fires. Evidence of arctic amplification may already be manifesting in Canada which contains 28% of the world's boreal zone (Walker *et al.*, 2019; Scholten *et al.*, 2021; Baron *et al.*, 2022; Descals *et al.*, 2022). Even before the record-breaking 2023 fire season of 17M ha, which more than doubled the previous high of 7M ha in 1995, and record high boreal fire emissions in 2021 (Zheng *et al.*, 2023), Canada already had more burned area and events, longer lasting and faster spreading fires than in other boreal countries from 2001-2020 (**Fig. 2**). Since 1959 the number of large fires (>200ha), burned area and fire season length have increased in Canada due to increases in fire weather indexes (Hanes *et al.*, 2019; Jones *et al.*, 2022). Meanwhile in Alaska, short-interval fires are increasing due to warming and increases in precipitation variability (Buma *et al.*, 2022), while shifts in species composition have been observed as species resilience to fire declines with climate change (Baltzer *et al.*, 2021). Many of the countries classified as boreal for this analysis also extend into the arctic, where increasing temperatures and aridity are making surface fuels more flammable (McCarty, Smith and Turetsky, 2020), resulting in increased burned area that is occurring earlier in the year and burning later into the growing season (McCarty *et al.*, 2021; Descals *et al.*, 2022).

National Policies Matter

The effects of climate are, however, muddled by policy, land change and management. In Canada, for instance, the expansion of the wildland urban interface has led to increased fire suppression efforts and lower burned area in the southern regions, while the less populated northern forests fires are largely unmanaged (Coops *et al.*, 2018). A warming climate also means opportunities for expanded agricultural production in boreal regions, which is likely to affect fire regimes.

Bolivia's changing fire regimes are another example where policy-driven chances in land use confound interactions between climate and fire. Fire has been used as a cultural tool in Bolivia for at least 4,500 years (Maezumi *et al.*, 2022) via slash-and-burn practices and occurring during the annual burning season (Killeen *et al.*, 2008). Since the turn of the century, Bolivia has experienced hotter and drier conditions along with complex, non-linear changes in land use that are uneven in space (**Fig. S3**), and correspond to changing policies and development (Devisscher *et al.*, 2016; Gautreau and Bruslé, 2019). Bolivia experienced severe droughts in 2010, 2016, and 2019 (**Fig. S3c**) (Lewis *et al.*, 2011; Brando *et al.*, 2014), and the length of Bolivia's fire season has increased since 2003 ($p < 0.05$, **Fig. S3**). Policy changes in 2009 geared towards doubling agricultural production have expanded the agricultural frontier, accounting for 77% of Bolivia's carbon emissions during that time (Redo, Millington and Hindery, 2011). On the other hand, Bolivia has large protected areas that have remained comparatively intact and free of fire. Therefore, while nation-wide trends in fire regime components are neutral when averaged across the country, local anecdotes suggest unprecedented changes in fire activity, and policy changes affecting fire activity that have taken place in the midst of our time series make it difficult to detect changes.

Study limitations

The results presented here depend on how accurately the FIREDpy algorithm delineates events, and how accurately the MODIS MCD64 burned area product classifies burned pixels and estimates their burn date. The MODIS burned area product is accurate for large fire events. For example, when Landsat-derived fire perimeters from the Monitoring Trends in Burn Severity Database (MTBS) (Eidenshink *et al* 2007) were spatially and temporally matched to FIREDpy-delineated perimeters, the regression of the sizes of paired events had an R^2 value of 0.92, and much of the remaining uncertainty had to do with biases inherent to the MTBS product (Balch *et al* 2020). The MCD64 burned area product has a pixel size of about 21 ha, and commission and omission errors were minimized for fires of at least 10 ha (Giglio *et al* 2018), so very small fires like those in single fields or small lightning ignitions that do not spread, will be missed. The other type of uncertainty is on the choice of spatial and temporal parameters of the moving window that is used in the FIREDpy algorithm to group pixels into events (see Balch *et al.* 2020 and Mahood *et al.* 2022 for a more detailed discussion). Selecting too narrow of a window can result in single events being divided into multiple events, and too wide of a window can result in over-aggregation. Which of these issues is more prevalent tends to follow biophysical gradients. Areas with less frequent, but larger events (e.g. the western U.S.) tend to be vulnerable to over-splitting (Balch *et al.*, 2020). Areas with frequent, small fires and high total burned area (e.g. tropical savannas) are more vulnerable to over-aggregation. This is a conceptually easy problem to validate quantitatively, but in practice it is difficult because most countries do not have independently-created burn perimeters based on Landsat—the US is a rare case. Therefore, for countries without validation data, Mahood *et al.* (2022) started with a plausible window size based on prior research (e.g. (Archibald *et al.*, 2009; Balch *et al.*, 2013; Frantz *et al.*, 2016; Andela *et al.*, 2018; Artés *et al.*, 2019)), visually inspected the fire event products once they were created, looked for evidence of over-aggregation and over-splitting, and adjusted the parameters if necessary. Because the moving window parameters varied by country, we avoided any direct statistical comparison of the fire regime attributes by country, and grouped by country in our mixed model analysis.

Conclusion

It is becoming increasingly recognized that managing fires from a fire regime perspective will be essential to adapt to future climate (Cochrane and Bowman, 2021; Kelly *et al.*, 2023). Extreme fire events, in particular fast-spreading events, cause the most socioeconomic impact, and policies that impact fire activity are, by and large, enacted and implemented at the national scale. In order to craft effective policies that protect people from fires, we need to better understand their fine- and coarse-scale spatial and temporal drivers. While most of the literature on global fire activity is centered around burned area and changes in the fire season, we found that the properties of events, especially growth rate and size, were mostly unrelated to country-wide burned area, number of fires, and fire season length. Because fire size and growth rate are driven by different climatic and social forces than burned area, it is crucial to incorporate local, place-based knowledge of policies and processes that drive the complex interplay between climate, fuels and ignitions that govern fire regimes. Such a nuanced understanding will be crucial for adapting to expected increases in fire activity and changing fire regimes.

Figures and Tables

Table 1. Total number of regions with positive, negative and neutral trends ($p < 0.05$) according to median-based regression models for each fire regime characteristic for the 145 countries with sufficient fire activity to analyze trends.

Climate Region	Fire Regime Component	Positive Trends	Negative Trends	Not Significant	% Positive	% Negative
Arid	Duration	12	19	40	17	27
	Mean Growth	16	23	32	23	32
	Max Growth	15	26	30	21	37
Event-Based	Size	15	27	29	21	38
Area-Based	N Fires	12	26	33	17	37
	Peak Season	12	12	47	17	17
	Season Length	28	11	31	40	16
	Burned Area	9	32	30	13	45
Boreal	Duration	5	12	32	10	24
	Mean Growth	6	13	30	12	27
	Max Growth	8	11	30	16	22
Event-Based	Size	6	8	35	12	16
Area-Based	N Fires	5	20	24	10	41
	Peak Season	10	5	34	20	10
	Season Length	6	6	37	12	12
	Burned Area	5	17	27	10	35
Equatorial	Duration	13	17	38	19	25
	Mean Growth	10	32	26	15	47
	Max Growth	9	28	31	13	41
Event-Based	Size	14	28	26	21	41
Area-Based	N Fires	9	28	31	13	41
	Peak Season	15	18	35	22	26
	Season Length	15	16	37	22	24
	Burned Area	5	36	27	7	53
Temperate	Duration	19	18	43	24	22
	Mean Growth	17	22	41	21	28
	Max Growth	15	24	41	19	30
Event-Based	Size	21	20	39	26	25
Area-Based	N Fires	11	30	39	14	38
	Peak Season	19	10	51	24	12
	Season Length	22	10	48	28	12
	Burned Area	11	33	36	14	41

All Regions	Duration	49	66	153	18	25
	Mean Growth	49	90	129	18	34
	Max Growth	47	89	132	18	33
Event-Based	Size	56	83	129	21	31
Area-Based	N Fires	37	104	127	14	39
	Peak Season	56	45	167	21	17
	Season Length	71	43	153	27	16
	Burned Area	30	118	120	11	44

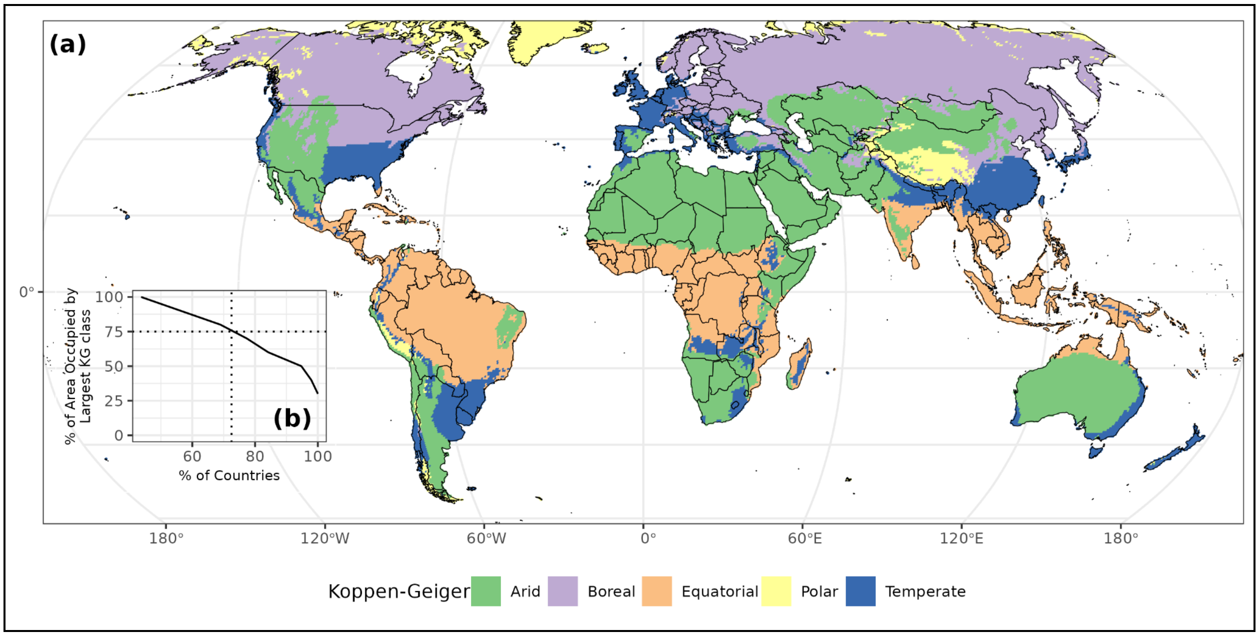

Figure 1. **Coarse Köppen-Geiger climate classifications** (Beck *et al.* 2018). Most (72%) countries have at least 75% of their land area covered by one class.

(a) Area-Based Attributes

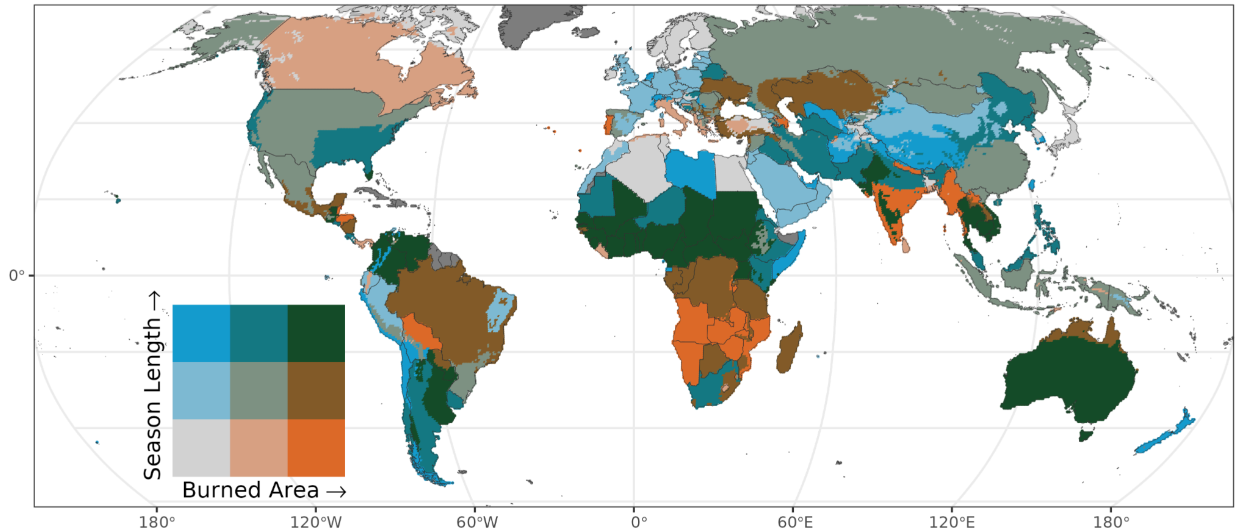

(b) Event-Based Attributes

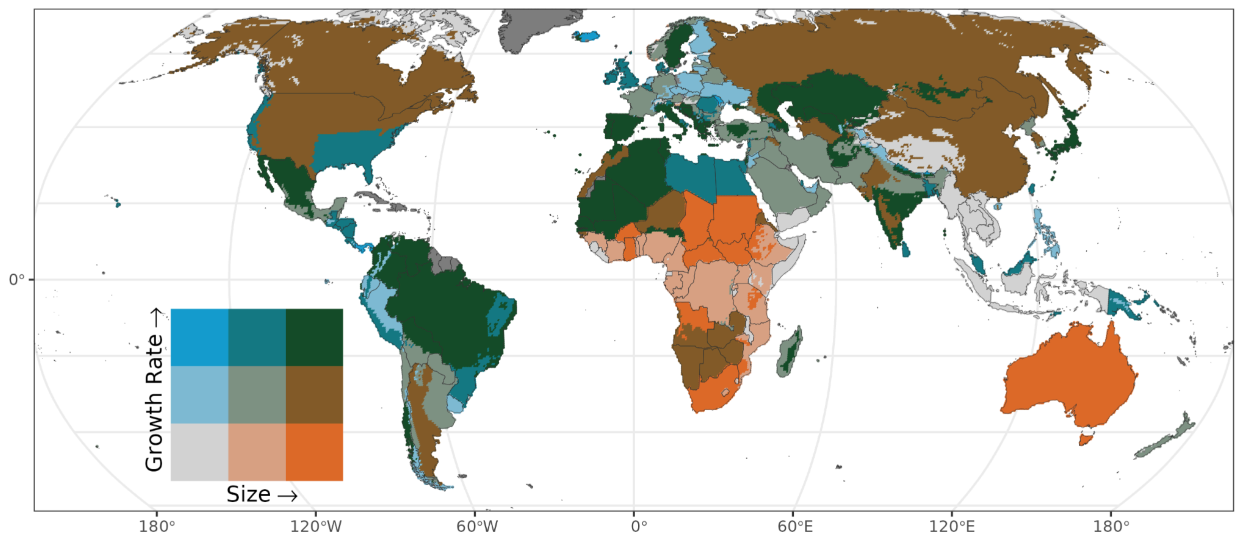

Figure 2. Spatial patterns in event- and area-based fire regime attributes ranked by quantiles. In (a), burned area and season length, representing the two main axes of variation for fire activity, are mapped. In (b), mean fire growth rate and number of fires are shown. Burned area and number of fires are standardized by the size of the country. Continuous variables were classified by 33rd and 66th quantiles.

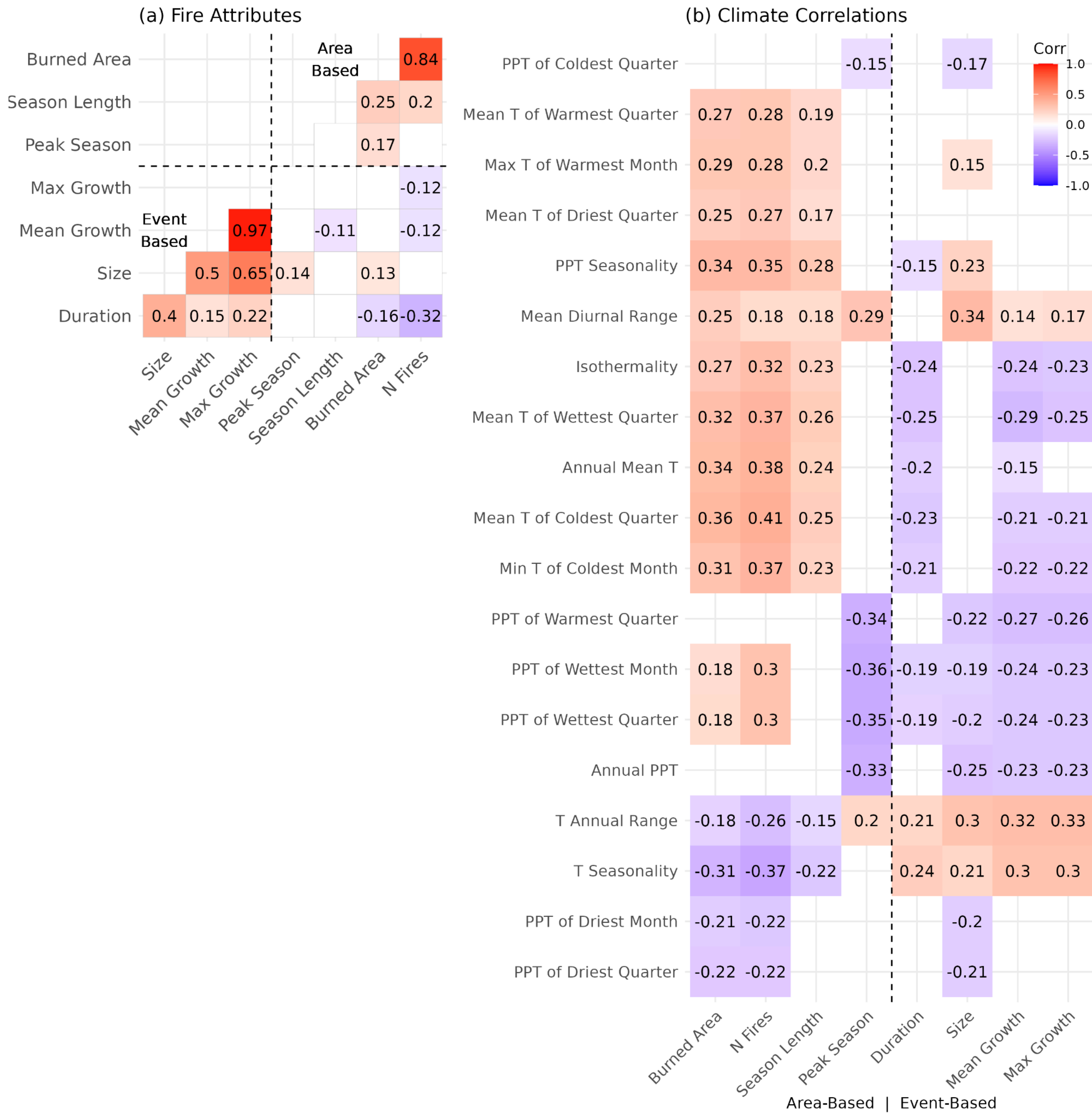
(a) Fire Attributes
Area Based
Event Based
Burned Area
Season Length
Peak Season
Max Growth
Mean Growth
Size
Duration
0.84
0.25 0.2
0.17
-0.12
0.97 -0.11 -0.12
0.5 0.65 0.14 0.13
0.4 0.15 0.22 -0.16 -0.32
Size
Mean Growth
Max Growth
Peak Season
Season Length
Burned Area
N Fires
(b) Climate Correlations
Corr
1.0
0.5
0.0
-0.5
-1.0
PPT of Coldest Quarter
Mean T of Warmest Quarter
Max T of Warmest Month
Mean T of Driest Quarter
PPT Seasonality
Mean Diurnal Range
Isothermality
Mean T of Wettest Quarter
Annual Mean T
Mean T of Coldest Quarter
Min T of Coldest Month
PPT of Warmest Quarter
PPT of Wettest Month
PPT of Wettest Quarter
Annual PPT
T Annual Range
T Seasonality
PPT of Driest Month
PPT of Driest Quarter
-0.15 -0.17
0.27 0.28 0.19
0.29 0.28 0.2 0.15
0.25 0.27 0.17
0.34 0.35 0.28 -0.15 0.23
0.25 0.18 0.18 0.29 0.34 0.14 0.17
0.27 0.32 0.23 -0.24 -0.24 -0.23
0.32 0.37 0.26 -0.25 -0.29 -0.25
0.34 0.38 0.24 -0.2 -0.15
0.36 0.41 0.25 -0.23 -0.21 -0.21
0.31 0.37 0.23 -0.21 -0.22 -0.22
-0.34 -0.22 -0.27 -0.26
0.18 0.3 -0.36 -0.19 -0.19 -0.24 -0.23
0.18 0.3 -0.35 -0.19 -0.2 -0.24 -0.23
-0.33 -0.25 -0.23 -0.23
-0.18 -0.26 -0.15 0.2 0.21 0.3 0.32 0.33
-0.31 -0.37 -0.22 0.24 0.21 0.3 0.3
-0.21 -0.22 -0.2
-0.22 -0.22 -0.21
Burned Area
N Fires
Season Length
Peak Season
Duration
Size
Mean Growth
Max Growth
Area-Based | Event-Based

Figure 3. Significant ($p < 0.05$) correlations among fire regime attributes (a) and between fire regime attributes and climate normals from WorldClim (b). Event-based characteristics were weakly related to area-based characteristics (a), and driven by different aspects of climate (b). The number in each square is the correlation coefficient. Note, burned area and number of fires are standardized by the size of the country. Abbreviations: T = temperature, PPT = precipitation.

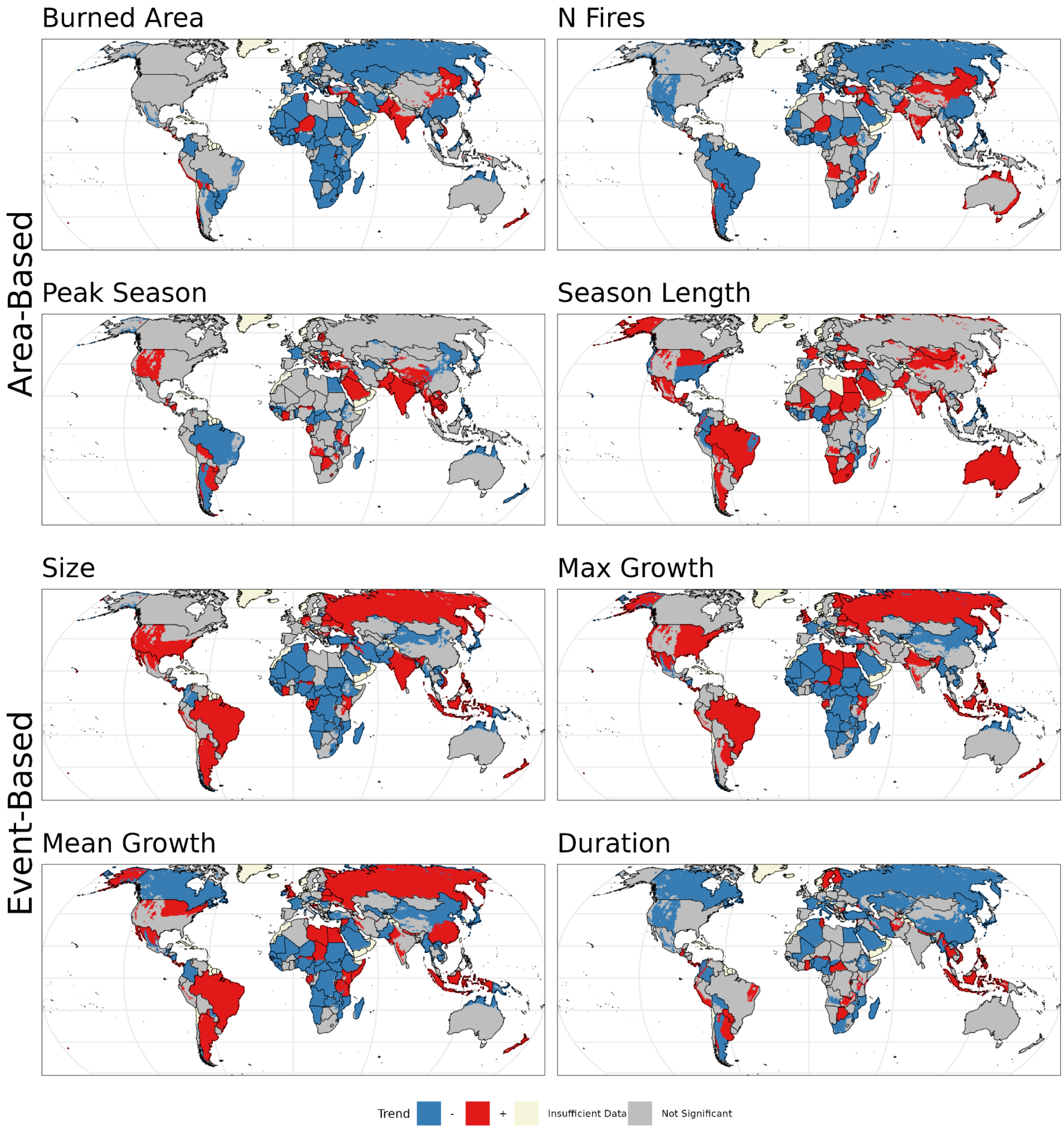

Figure 4. Annual trends in each fire regime characteristic by Köppen-Geiger climate region and country according to median-based linear regression ($p < 0.05$).

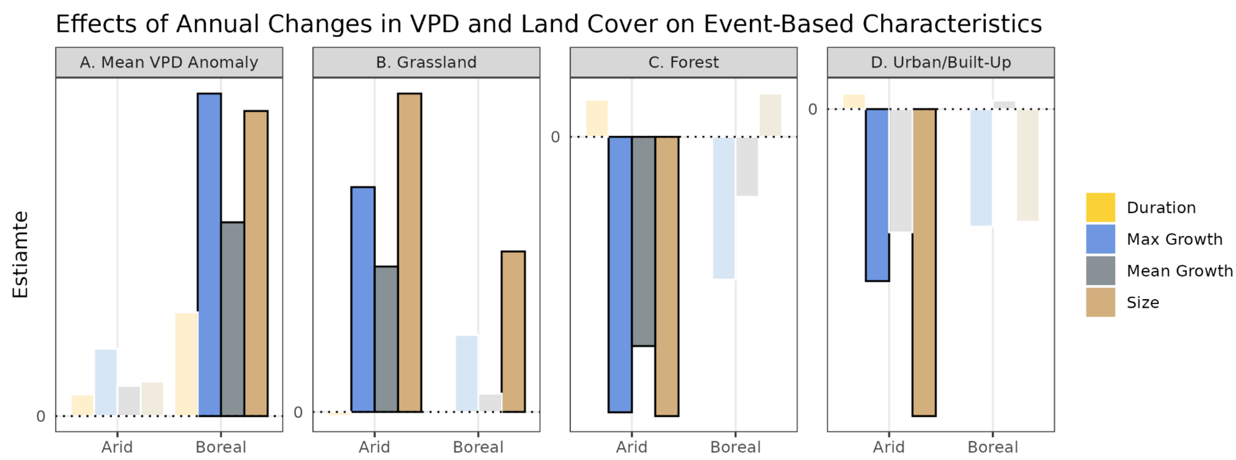

Figure 5. Changes in size and growth rate followed expectations of fuel versus energy limitations in arid and boreal regions. Associations of annual changes in land cover and vapor pressure deficit with event-based fire regime characteristics for boreal regions with 43 countries and arid regions in 70 countries where there was fire activity in more than 15 years from 2003-2020. Darker-colored, outlined bars represent statistically significant relationships ($p < 0.05$).

References

Abatzoglou, J.T. *et al.* (2018) “TerraClimate, a high-resolution global dataset of monthly climate and climatic water balance from 1958–2015,” *Scientific Data*, 5(1), p. 170191. Available at: https://doi.org/10.1038/sdata.2017.191.

Abatzoglou, J.T. and Williams, A.P. (2016) “Impact of anthropogenic climate change on wildfire across western US forests,” *Proceedings of the National Academy of Sciences*, 113(42), pp. 11770–11775. Available at: https://doi.org/10.1073/pnas.1607171113.

Andela, N. *et al.* (2017) “A human-driven decline in global burned area,” *Science*, 356(6345), pp. 1356–1362. Available at: https://doi.org/10.1126/science.aal4108.

Andela, N. *et al.* (2018) *The Global Fire Atlas of individual fire size, duration, speed, and direction*. preprint. Biosphere – Biogeosciences. Available at: https://doi.org/10.5194/essd-2018-89.

Anderson, D.B. (1936) “Relative Humidity or Vapor Pressure Deficit,” *Ecology*, 17(2), pp. 277–282. Available at: https://doi.org/10.2307/1931468.

Archibald, S. *et al.* (2009) “What limits fire? An examination of drivers of burnt area in Southern Africa,” *Global Change Biology*, 15(3), pp. 613–630. Available at: https://doi.org/10.1111/j.1365-2486.2008.01754.x.

Archibald, S. *et al.* (2013) “Defining pyromes and global syndromes of fire regimes,” *Proceedings of the National Academy of Sciences*, 110(16), pp. 6442–6447. Available at: https://doi.org/10.1073/pnas.1211466110.

Artés, T. *et al.* (2019) “A global wildfire dataset for the analysis of fire regimes and fire behaviour,” *Scientific Data*, 6(1), p. 296. Available at: https://doi.org/10.1038/s41597-019-0312-2.

Balch, J.K. *et al.* (2013) “Introduced annual grass increases regional fire activity across the arid western USA (1980–2009),” *Global Change Biology*, 19(1), pp. 173–183. Available at: https://doi.org/10.1111/gcb.12046.

Balch, J.K. *et al.* (2016) “Global combustion: the connection between fossil fuel and biomass burning emissions (1997–2010),” *Philosophical Transactions of the Royal Society B: Biological Sciences*, 371(1696), p. 20150177. Available at: https://doi.org/10.1098/rstb.2015.0177.

Balch, J.K. *et al.* (2017) “Human-started wildfires expand the fire niche across the United States,” *Proceedings of the National Academy of Sciences*, 114(11), pp. 2946–2951. Available at: https://doi.org/10.1073/pnas.1617394114.

Balch, J.K. *et al.* (2020) “FIRED (Fire Events Delineation): An Open, Flexible Algorithm and Database of US Fire Events Derived from the MODIS Burned Area Product (2001–2019),” *Remote Sensing*, 12(21), p. 3498. Available at: https://doi.org/10.3390/rs12213498.

Balch, J.K. *et al.* (2022) “Warming weakens the night-time barrier to global fire,” *Nature*, 602(7897), pp. 442–448. Available at: https://doi.org/10.1038/s41586-021-04325-1.

Balch, J.K. *et al.* (2024) “The fastest-growing and most destructive fires in the US (2001 to 2020),” *Science*, 386(6720), pp. 425–431. Available at: https://doi.org/10.1126/science.adk5737.

Balik, J.A. *et al.* (2024) “Biogeographic patterns of daily wildfire spread and extremes across North America,” *Frontiers in Forests and Global Change*, 7, p. 1355361. Available at: https://doi.org/10.3389/ffgc.2024.1355361.

Baltzer, J.L. *et al.* (2021) “Increasing fire and the decline of fire adapted black spruce in the boreal forest,” *Proceedings of the National Academy of Sciences*, 118(45), p. e2024872118. Available at: https://doi.org/10.1073/pnas.2024872118.

Barber, Q.E. *et al.* (2024) “The Canadian Fire Spread Dataset,” *Scientific Data*, 11(1), p. 764. Available at: https://doi.org/10.1038/s41597-024-03436-4.

Baron, J.N. *et al.* (2022) “A century of transformation: fire regime transitions from 1919 to 2019 in southeastern British Columbia, Canada,” *Landscape Ecology*, 37(10), pp. 2707–2727. Available at: https://doi.org/10.1007/s10980-022-01506-9.

Bates, D. *et al.* (2015) “Fitting Linear Mixed-Effects Models Using **lme4**,” *Journal of Statistical Software*, 67(1). Available at: https://doi.org/10.18637/jss.v067.i01.

Beck, H.E. *et al.* (2018) “Present and future Köppen-Geiger climate classification maps at 1-km resolution,” *Scientific Data*, 5(1), p. 180214. Available at: https://doi.org/10.1038/sdata.2018.214.

Bennett, M.M. *et al.* (2022) “The politics of pixels: A review and agenda for critical remote sensing,” *Progress in Human Geography*, 46(3), pp. 729–752. Available at: https://doi.org/10.1177/03091325221074691.

Brando, P.M. *et al.* (2014) “Abrupt increases in Amazonian tree mortality due to drought-fire interactions,” *Proceedings of the National Academy of Sciences*, 111(17), pp. 6347–6352. Available at: https://doi.org/10.1073/pnas.1305499111.

Brown, P.T. *et al.* (2023) “Climate warming increases extreme daily wildfire growth risk in California,” *Nature*, 621(7980), pp. 760–766. Available at: https://doi.org/10.1038/s41586-023-06444-3.

Buma, B. *et al.* (2022) “Short-interval fires increasing in the Alaskan boreal forest as fire self-regulation decays across forest types,” *Scientific Reports*, 12(1), p. 4901. Available at: https://doi.org/10.1038/s41598-022-08912-8.

Cattau, M.E. *et al.* (2016) “Sources of anthropogenic fire ignitions on the peat-swamp landscape in Kalimantan, Indonesia,” *Global Environmental Change*, 39, pp. 205–219. Available at: https://doi.org/10.1016/j.gloenvcha.2016.05.005.

Cattau, M.E. *et al.* (2020) “Anthropogenic and lightning‐started fires are becoming larger and more frequent over a longer season length in the U.S.A.,” *Global Ecology and Biogeography*. Edited by B. Poulter, 29(4), pp. 668–681. Available at: https://doi.org/10.1111/geb.13058.

Cattau, M.E. *et al.* (2022) “Modern Pyromes: Biogeographical Patterns of Fire Characteristics across the Contiguous United States,” *Fire*, 5(4), p. 95. Available at: https://doi.org/10.3390/fire5040095.

Chen, Y. *et al.* (2023) “Multi-decadal trends and variability in burned area from the fifth version of the Global Fire Emissions Database (GFED5),” *Earth System Science Data*, 15(11), pp. 5227–5259. Available at: https://doi.org/10.5194/essd-15-5227-2023.

Cochrane, M.A. and Bowman, D.M. (2021) “Manage fire regimes, not fires,” *Nature Geoscience*, 14(7), pp. 455–457. Available at: https://doi.org/10.1038/s41561-021-00791-4.

Collins, S.L. *et al.* (2021) “Fire frequency, state change and hysteresis in tallgrass prairie,” *Ecology Letters*. Edited by L. Comita, 24(4), pp. 636–647. Available at: https://doi.org/10.1111/ele.13676.

Coop, J.D. *et al.* (2022) “Extreme fire spread events and area burned under recent and future climate in the western USA," *Global Ecology and Biogeography*, 31(10), pp. 1949–1959. Available at: https://doi.org/10.1111/geb.13496.

Coops, N.C. *et al.* (2018) "A thirty year, fine-scale, characterization of area burned in Canadian forests shows evidence of regionally increasing trends in the last decade," *PLOS ONE*. Edited by E.G. Lamb, 13(5), p. e0197218. Available at: https://doi.org/10.1371/journal.pone.0197218.

Cunningham, C.X., Williamson, G.J. and Bowman, D.M.J.S. (2024) "Increasing frequency and intensity of the most extreme wildfires on Earth," *Nature Ecology & Evolution* [Preprint]. Available at: https://doi.org/10.1038/s41559-024-02452-2.

Dennison, P.E. *et al.* (2014) "Large wildfire trends in the western United States," *Geophysical Research Letters*, 41(8), pp. 2928–2933. Available at: https://doi.org/10.1002/2014GL059576.

Descals, A. *et al.* (2022) "Unprecedented fire activity above the Arctic Circle linked to rising temperatures," *Science*, 378(6619), pp. 532–537. Available at: https://doi.org/10.1126/science.abn9768.

Devisscher, T. *et al.* (2016) "Increased Wildfire Risk Driven by Climate and Development Interactions in the Bolivian Chiquitania, Southern Amazonia," *PLOS ONE*. Edited by J. Mpodozis, 11(9), p. e0161323. Available at: https://doi.org/10.1371/journal.pone.0161323.

Earl, N. and Simmonds, I. (2018) "Spatial and Temporal Variability and Trends in 2001–2016 Global Fire Activity," *Journal of Geophysical Research: Atmospheres*, 123(5), pp. 2524–2536. Available at: https://doi.org/10.1002/2017JD027749.

Eidenshink, J. *et al.* (2007) "A Project for Monitoring Trends in Burn Severity," *Fire Ecology*, 3(1), pp. 3–21. Available at: https://doi.org/10.4996/fireecology.0301003.

Fick, S.E. and Hijmans, R.J. (2017) "WorldClim 2: new 1-km spatial resolution climate surfaces for global land areas," *International journal of climatology*, 37(12), pp. 4302–4315.

Frantz, D. *et al.* (2016) "Fire spread from MODIS burned area data: obtaining fire dynamics information for every single fire," *International Journal of Wildland Fire*, 25(12), p. 1228. Available at: https://doi.org/10.1071/WF16003.

Fusco, E.J. *et al.* (2019) "Invasive grasses increase fire occurrence and frequency across US ecoregions," *Proceedings of the National Academy of Sciences*, 116(47), pp. 23594–23599. Available at: https://doi.org/10.1073/pnas.1908253116.

Fusco, E.J. *et al.* (2021) "The human–grass–fire cycle: how people and invasives co-occur to drive fire regimes," *Frontiers in Ecology and the Environment*, p. fee.2432. Available at: https://doi.org/10.1002/fee.2432.

García, M. *et al.* (2022) "Characterizing Global Fire Regimes from Satellite-Derived Products," *Forests*, 13(5), p. 699. Available at: https://doi.org/10.3390/f13050699.

Gautreau, P. and Bruslé, L.P. (2019) "Forest management in Bolivia under Evo Morales: The challenges of post-neoliberalism," *Political Geography*, 68, pp. 110–121. Available at: https://doi.org/10.1016/j.polgeo.2018.12.003.

Giglio, L. *et al.* (2018) “The Collection 6 MODIS burned area mapping algorithm and product,” *Remote Sensing of Environment*, 217, pp. 72–85. Available at: https://doi.org/10.1016/j.rse.2018.08.005.

Giglio, L., Randerson, J.T. and Van Der Werf, G.R. (2013) “Analysis of daily, monthly, and annual burned area using the fourth‐generation global fire emissions database (GFED4),” *Journal of Geophysical Research: Biogeosciences*, 118(1), pp. 317–328.

Griebel, A. *et al.* (2023) “Specific leaf area and vapour pressure deficit control live fuel moisture content,” *Functional Ecology*, 37(3), pp. 719–731. Available at: https://doi.org/10.1111/1365-2435.14271.

Grossiord, C. *et al.* (2020) “Plant responses to rising vapor pressure deficit,” *New Phytologist*, 226(6), pp. 1550–1566. Available at: https://doi.org/10.1111/nph.16485.

Grünig, M., Seidl, R. and Senf, C. (2023) “Increasing aridity causes larger and more severe forest fires across Europe,” *Global Change Biology*, 29(6), pp. 1648–1659. Available at: https://doi.org/10.1111/gcb.16547.

Hanes, C.C. *et al.* (2019) “Fire-regime changes in Canada over the last half century,” *Canadian Journal of Forest Research*, 49(3), pp. 256–269. Available at: https://doi.org/10.1139/cjfr-2018-0293.

Hantson, S. *et al.* (2022) “Human-ignited fires result in more extreme fire behavior and ecosystem impacts,” *Nature Communications*, 13(1), p. 2717. Available at: https://doi.org/10.1038/s41467-022-30030-2.

Heenatigala, M. (2021) *Influence of Climate Change on Forest Fire Occurrence and Distribution of Sri Lanka and Modeling of Forest Fire*. Portland State University. Available at: https://doi.org/10.15760/mem.71.

Higuera, P.E. *et al.* (2023) “Shifting social-ecological fire regimes explain increasing structure loss from Western wildfires,” *PNAS Nexus*. Edited by J. Liu, 2(3), p. pgad005. Available at: https://doi.org/10.1093/pnasnexus/pgad005.

Iglesias, V., Balch, J.K. and Travis, W.R. (2022) “U.S. fires became larger, more frequent, and more widespread in the 2000s,” *Science Advances*, 8(11), p. eabc0020. Available at: https://doi.org/10.1126/sciadv.abc0020.

Jolly, W.M. *et al.* (2015) “Climate-induced variations in global wildfire danger from 1979 to 2013,” *Nature Communications*, 6(1), p. 7537. Available at: https://doi.org/10.1038/ncomms8537.

Jones, G.M. *et al.* (2021) “Megafire causes persistent loss of an old‐forest species,” *Animal Conservation*, 24(6), pp. 925–936. Available at: https://doi.org/10.1111/acv.12697.

Jones, M.W. *et al.* (2022) “Global and Regional Trends and Drivers of Fire Under Climate Change,” *Reviews of Geophysics*, 60(3). Available at: https://doi.org/10.1029/2020RG000726.

Kasoar, M. *et al.* (2024) “Model fires, not ignitions: Capturing the human dimension of global fire regimes,” *Cell Reports Sustainability*, 1(6), p. 100128. Available at: https://doi.org/10.1016/j.crsus.2024.100128.

Keeley, J.E. and Pausas, J.G. (2019) “Distinguishing disturbance from perturbations in fire-prone ecosystems,” *International Journal of Wildland Fire*, 28(4), p. 282. Available at: https://doi.org/10.1071/WF18203.

Kelley, D.I. *et al.* (2019) “How contemporary bioclimatic and human controls change global fire regimes,” *Nature Climate Change*, 9(9), pp. 690–696. Available at: https://doi.org/10.1038/s41558-019-0540-7.

Kelly, L.T. *et al.* (2023) “Understanding Fire Regimes for a Better Anthropocene,” *Annual Review of Environment and Resources*, 48(1), pp. 207–235. Available at: https://doi.org/10.1146/annurev-environ-120220-055357.

Kelso, N.V. and Patterson, T. (2010) “Introducing natural earth data-naturalearthdata. com,” *Geographia Technica*, 5(82–89), p. 25.

Killeen, T.J. *et al.* (2008) “Total Historical Land-Use Change in Eastern Bolivia: Who, Where, When, and How Much?,” *Ecology and Society*, 13(1), p. art36. Available at: https://doi.org/10.5751/ES-02453-130136.

Krawchuk, M.A. and Moritz, M.A. (2011) “Constraints on global fire activity vary across a resource gradient,” *Ecology*, 92(1), pp. 121–132. Available at: https://doi.org/10.1890/09-1843.1.

Lewis, S.L. *et al.* (2011) “The 2010 Amazon Drought,” *Science*, 331(6017), pp. 554–554. Available at: https://doi.org/10.1126/science.1200807.

Luo, K. *et al.* (2024) “Drought triggers and sustains overnight fires in North America,” *Nature*, 627(8003), pp. 321–327. Available at: https://doi.org/10.1038/s41586-024-07028-5.

Maezumi, S.Y. *et al.* (2022) “Legacies of Indigenous land use and cultural burning in the Bolivian Amazon rainforest ecotone,” *Philosophical Transactions of the Royal Society B: Biological Sciences*, 377(1849), p. 20200499. Available at: https://doi.org/10.1098/rstb.2020.0499.

Mahood, A.L. *et al.* (2022) “Country-level fire perimeter datasets (2001–2021),” *Scientific Data*, 9(1), p. 458. Available at: https://doi.org/10.1038/s41597-022-01572-3.

Mahood, A.L., Koontz, M.J. and Balch, J.K. (2023) “Fuel connectivity, burn severity, and seed bank survivorship drive ecosystem transformation in a semiarid shrubland,” *Ecology* [Preprint]. Available at: https://doi.org/10.1002/ecy.3968.

McCarty, J.L. *et al.* (2021) “Reviews and syntheses: Arctic fire regimes and emissions in the 21st century,” *Biogeosciences*, 18(18), pp. 5053–5083. Available at: https://doi.org/10.5194/bg-18-5053-2021.

McCarty, J.L., Smith, T.E.L. and Turetsky, M.R. (2020) “Arctic fires re-emerging,” *Nature Geoscience*, 13(10), pp. 658–660. Available at: https://doi.org/10.1038/s41561-020-00645-5.

Moritz, M.A. *et al.* (2012) “Climate change and disruptions to global fire activity,” *Ecosphere*, 3(6), p. art49. Available at: https://doi.org/10.1890/ES11-00345.1.

Novick, K.A. *et al.* (2024) “The impacts of rising vapour pressure deficit in natural and managed ecosystems,” *Plant, Cell & Environment*, p. pce.14846. Available at:

https://doi.org/10.1111/pce.14846.

Pais, C. *et al.* (2023) “Global scale coupling of pyromes and fire regimes,” *Communications Earth & Environment*, 4(1), p. 267. Available at: https://doi.org/10.1038/s43247-023-00881-8.

Redo, D., Millington, A.C. and Hindery, D. (2011) “Deforestation dynamics and policy changes in Bolivia’s post-neoliberal era,” *Land Use Policy*, 28(1), pp. 227–241. Available at: https://doi.org/10.1016/j.landusepol.2010.06.004.

Resco De Dios, V. *et al.* (2022) “Convergence in critical fuel moisture and fire weather thresholds associated with fire activity in the pyroregions of Mediterranean Europe,” *Science of The Total Environment*, 806, p. 151462. Available at: https://doi.org/10.1016/j.scitotenv.2021.151462.

Scholten, R.C. *et al.* (2021) “Overwintering fires in boreal forests,” *Nature*, 593(7859), pp. 399–404. Available at: https://doi.org/10.1038/s41586-021-03437-y.

Seager, R. *et al.* (2015) “Climatology, Variability, and Trends in the U.S. Vapor Pressure Deficit, an Important Fire-Related Meteorological Quantity,” *Journal of Applied Meteorology and Climatology*, 54(6), pp. 1121–1141. Available at: https://doi.org/10.1175/JAMC-D-14-0321.1.

Sedano, F. and Randerson, J.T. (2014) “Multi-scale influence of vapor pressure deficit on fire ignition and spread in boreal forest ecosystems,” *Biogeosciences*, 11(14), pp. 3739–3755. Available at: https://doi.org/10.5194/bg-11-3739-2014.

Serreze, M.C. and Barry, R.G. (2011) “Processes and impacts of Arctic amplification: A research synthesis,” *Global and Planetary Change*, 77(1–2), pp. 85–96. Available at: https://doi.org/10.1016/j.gloplacha.2011.03.004.

Siegel, A.F. (1982) “Robust Regression Using Repeated Medians,” *Biometrika*, 69(1), pp. 242–244.

Sloan, S. *et al.* (2022) “Declining severe fire activity on managed lands in Equatorial Asia,” *Communications Earth & Environment*, 3(1), p. 207. Available at: https://doi.org/10.1038/s43247-022-00522-6.

Stigler, S.M. (1989) “Francis Galton’s Account of the Invention of Correlation,” *Statistical Science*, 4(2). Available at: https://doi.org/10.1214/ss/1177012580.

Sugihara, N.G., Van Wagtendonk, J.W. and Fites-Kaufman, J. (2006) “58Fire as an Ecological Process,” in N. Sugihara (ed.) *Fire in California’s Ecosystems*. University of California Press, p. 0. Available at: https://doi.org/10.1525/california/9780520246058.003.0004.

Sulla-Menashe, D. and Friedl, M.A. (2018) “User guide to collection 6 MODIS land cover (MCD12Q1 and MCD12C1) product,” p. 18.

Taylor, A.H. *et al.* (2016) “Socioecological transitions trigger fire regime shifts and modulate fire–climate interactions in the Sierra Nevada, USA, 1600–2015 CE,” *Proceedings of the National Academy of Sciences*, 113(48), pp. 13684–13689. Available at: https://doi.org/10.1073/pnas.1609775113.

Vadrevu, K.P. *et al.* (2019) “Trends in Vegetation fires in South and Southeast Asian Countries,” *Scientific Reports*, 9(1), p. 7422. Available at: https://doi.org/10.1038/s41598-019-43940-x.

Vetrita, Y. and Cochrane, M.A. (2019) “Fire Frequency and Related Land-Use and Land-Cover Changes in Indonesia’s Peatlands,” *Remote Sensing*, 12(1), p. 5. Available at: https://doi.org/10.3390/rs12010005.

Walker, X.J. *et al.* (2019) “Increasing wildfires threaten historic carbon sink of boreal forest soils,” *Nature*, 572(7770), pp. 520–523. Available at: https://doi.org/10.1038/s41586-019-1474-y.

Ward, D.S. *et al.* (2018) “Trends and variability of global fire emissions due to historical anthropogenic activities,” *Global Biogeochemical Cycles*, 32(1), pp. 122–142.

White, P.S. and Jentsch, A. (2001) “The Search for Generality in Studies of Disturbance and Ecosystem Dynamics,” in K. Esser et al. (eds.) *Progress in Botany*. Berlin, Heidelberg: Springer Berlin Heidelberg (Progress in Botany), pp. 399–450. Available at: https://doi.org/10.1007/978-3-642-56849-7_17.

Whitman, E. *et al.* (2022) “Climate-induced fire regime amplification in Alberta, Canada,” *Environmental Research Letters*, 17(5), p. 055003. Available at: https://doi.org/10.1088/1748-9326/ac60d6.

Williams, A.P. *et al.* (2014) “Correlations between components of the water balance and burned area reveal new insights for predicting forest fire area in the southwest United States,” *International Journal of Wildland Fire*, 24(1), pp. 14–26.

Yuan, W. *et al.* (2019) “Increased atmospheric vapor pressure deficit reduces global vegetation growth,” *Science Advances*, 5(8), p. eaax1396. Available at: https://doi.org/10.1126/sciadv.aax1396.

Zhang, W. *et al.* (2025) “Global Fire Season Types and Their Characteristics Based on MODIS Burned Area Data,” *Chinese Geographical Science*, 35(2), pp. 374–383. Available at: https://doi.org/10.1007/s11769-025-1501-x.

Zheng, B. *et al.* (2023) “Record-high CO_2 emissions from boreal fires in 2021,” *Science*, 379(6635), pp. 912–917. Available at: https://doi.org/10.1126/science.ade0805.

Supplement for “The properties of individual fire events are essential for understanding global fire regimes”

Supplementary Figures

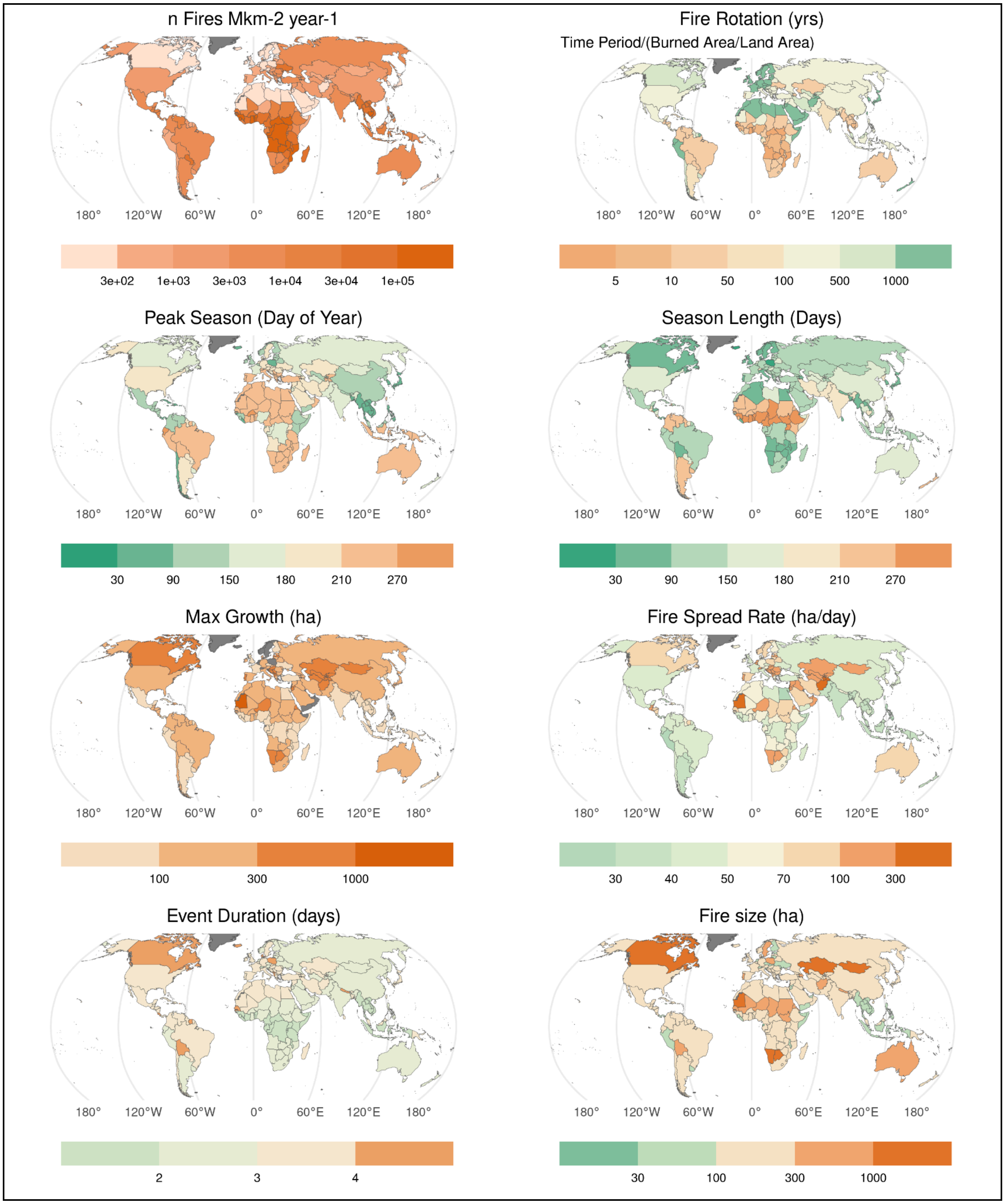

Figure S1. Spatial patterns of each fire characteristic by country.

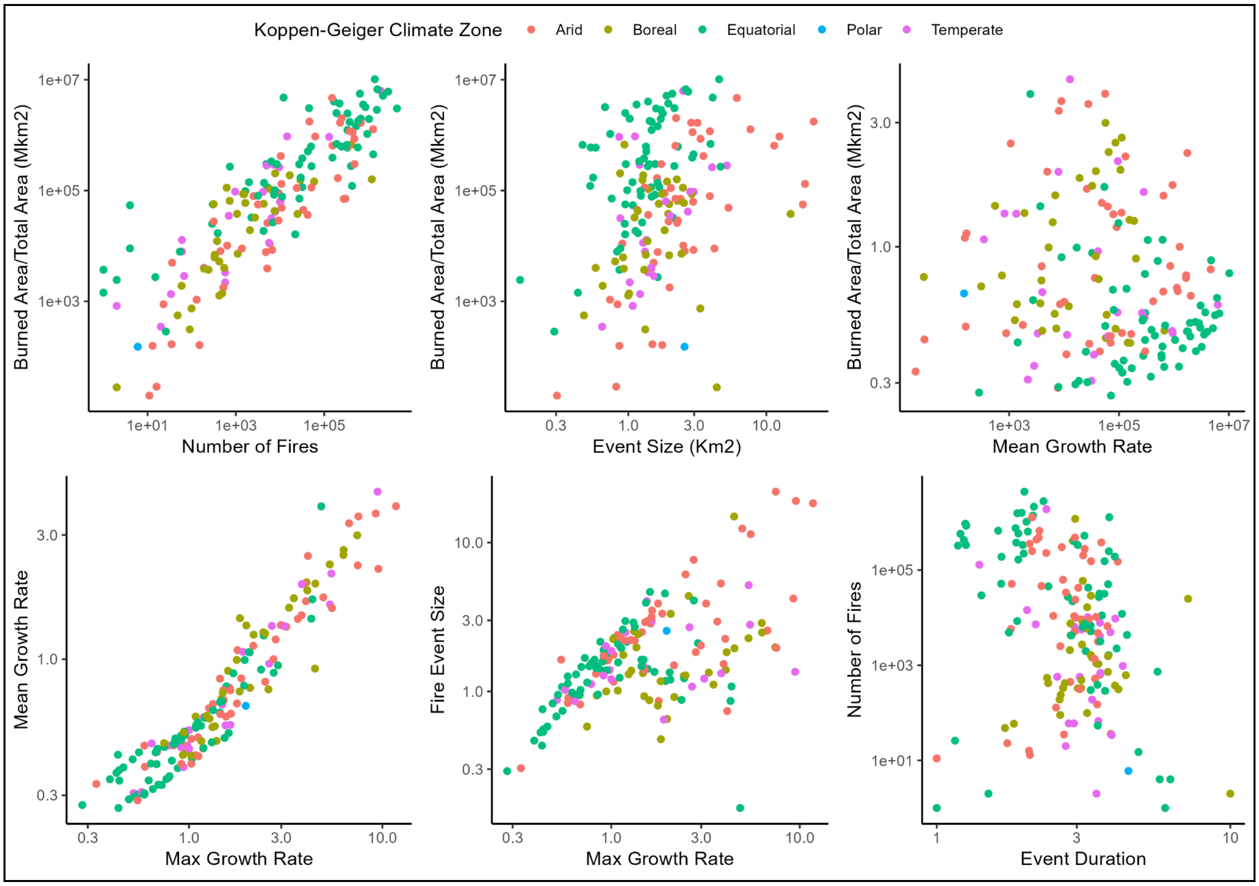

Figure S2. Burned area and number of fires are strongly related, as are growth rate and size.

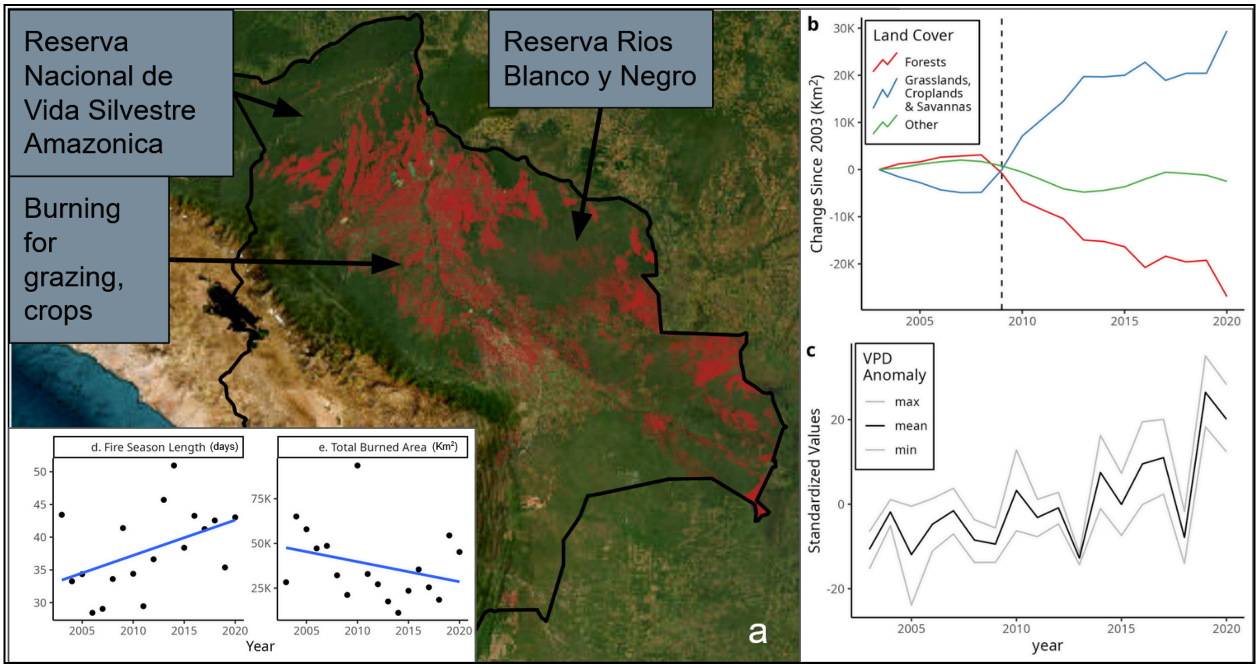

Figure S3. Bolivia exhibits a complex interplay between changes in land use and VPD that complicate the examination of national trends in fire regimes. Panel a shows the spatial distribution of fires (red), b shows temporal changes in land cover from the MODIS land cover product, with the dashed line indicating a policy change. Panel c shows the trend in vapor pressure deficit anomalies, d shows fire season length and e shows total burned area, all from 2003-2020.

Supplementary Tables

Table S1. Burned area of all countries, in order.

Country	Burned Area (km^2)	% Total	Cumulative %	Rank
Australia	9,810,000	11.58059	12	1
Angola	7,609,000	8.98234	21	2
Democratic Republic Of The Congo	7,050,000	8.32244	29	3
South Sudan	6,352,000	7.49846	36	4
Zambia	4,754,000	5.61204	42	5
Central African Republic	4,167,000	4.91909	47	6
Mozambique	4,058,000	4.79042	52	7
Brazil	3,818,000	4.5071	56	8
Tanzania	2,700,000	3.18732	59	9
Russia	2,683,000	3.16725	63	10
Chad	2,115,000	2.49673	65	11
Nigeria	1,783,000	2.10481	67	12
Kazakhstan	1,752,000	2.06822	69	13
Sudan	1,600,000	1.88878	71	14
Mali	1,480,000	1.74712	73	15
Ghana	1,341,000	1.58303	74	16
Ethiopia	1,279,000	1.50984	76	17
Botswana	1,018,000	1.20174	77	18
Senegal	922,000	1.08841	78	19
India	871,700	1.02903	79	20
Guinea	871,000	1.02821	80	21
Madagascar	859,500	1.01463	81	22
Cameroon	838,200	0.98949	82	23
Argentina	835,400	0.98618	83	24
South Africa	782,500	0.92373	84	25
Namibia	778,400	0.91889	85	26
Bolivia	754,600	0.8908	86	27
Myanmar	695,700	0.82127	87	28
Republic Of The Congo	687,200	0.81123	88	29
United States	666,100	0.78632	88	30
China	664,900	0.78491	89	31
Zimbabwe	652,000	0.76968	90	32
Uganda	596,300	0.70393	91	33
Cambodia	580,300	0.68504	91	34
Venezuela	566,300	0.66851	92	35
Ivory Coast	556,800	0.6573	93	36
Burkina Faso	555,400	0.65564	93	37
Paraguay	495,200	0.58458	94	38

Colombia	446,700	0.52732	94	39
Benin	433,200	0.51139	95	40
Ukraine	383,800	0.45307	95	41
Canada	372,900	0.4402	96	42
Mexico	328,100	0.38732	96	43
Thailand	308,400	0.36406	97	44
Togo	230,500	0.2721	97	45
Indonesia	226,600	0.2675	97	46
Mongolia	205,200	0.24224	97	47
Vietnam	194,900	0.23008	98	48
Sierra Leone	180,000	0.21249	98	49
Laos	152,200	0.17967	98	50
Turkey	113,200	0.13363	98	51
Malawi	111,100	0.13115	98	52
Guinea-Bissau	98,020	0.11571	98	53
Gabon	71,420	0.08431	99	54
Guatemala	67,450	0.07962	99	55
Kenya	67,440	0.07961	99	56
Iran	58,960	0.0696	99	57
Mauritania	58,090	0.06857	99	58
Niger	57,880	0.06833	99	59
Honduras	57,630	0.06803	99	60
Papua New Guinea	53,390	0.06303	99	61
Gambia	49,040	0.05789	99	62
Iraq	48,670	0.05745	99	63
Cuba	41,500	0.04899	99	64
Pakistan	39,090	0.04615	99	65
Nepal	38,660	0.04564	99	66
Nicaragua	38,420	0.04535	99	67
Romania	36,640	0.04325	99	68
Azerbaijan	36,230	0.04277	99	69
Turkmenistan	29,430	0.03474	99	70
Portugal	25,660	0.03029	99	71
Chile	21,210	0.02504	99	72
Bulgaria	21,180	0.025	100	73
Spain	21,020	0.02481	100	74
Peru	20,920	0.0247	100	75
Philippines	20,770	0.02452	100	76
Algeria	19,640	0.02318	100	77
Italy	19,120	0.02257	100	78
Syria	16,820	0.01986	100	79
Guyana	16,420	0.01938	100	80
Liberia	16,360	0.01931	100	81
Eswatini	16,120	0.01903	100	82
Greece	12,280	0.0145	100	83
Uzbekistan	11,650	0.01375	100	84
Bangladesh	11,380	0.01343	100	85
Eritrea	9,781	0.01155	100	86
Belarus	8,825	0.01042	100	87

Lesotho	8,729	0.0103	100	88
Malaysia	8,673	0.01024	100	89
Serbia	8,234	0.00972	100	90
Burundi	8,122	0.00959	100	91
Egypt	7,768	0.00917	100	92
Belize	7,627	0.009	100	93
Rwanda	7,616	0.00899	100	94
Sri Lanka	7,554	0.00892	100	95
Saudi Arabia	7,533	0.00889	100	96
Panama	7,503	0.00886	100	97
France	7,218	0.00852	100	98
Costa Rica	7,071	0.00835	100	99
North Korea	7,052	0.00832	100	100
Moldova	6,756	0.00798	100	101
Afghanistan	5,751	0.00679	100	102
Uruguay	5,600	0.00661	100	103
Somalia	5,232	0.00618	100	104
Ecuador	4,768	0.00563	100	105
Suriname	4,736	0.00559	100	106
Bosnia And Herzegovina	4,454	0.00526	100	107
Georgia	4,129	0.00487	100	108
Dominican Republic	3,905	0.00461	100	109
Kyrgyzstan	3,812	0.0045	100	110
The Bahamas	3,408	0.00402	100	111
Hungary	3,018	0.00356	100	112
Albania	2,706	0.00319	100	113
Japan	2,670	0.00315	100	114
Armenia	2,559	0.00302	100	115
East Timor	2,119	0.0025	100	116
Croatia	2,066	0.00244	100	117
El Salvador	1,993	0.00235	100	118
Republic Of Macedonia	1,648	0.00195	100	119
Tunisia	1,587	0.00187	100	120
Montenegro	1,535	0.00181	100	121
Bhutan	1,396	0.00165	100	122
Tajikistan	1,144	0.00135	100	123
Morocco	1,037	0.00122	100	124
United Kingdom	795.6	0.00094	100	125
South Korea	656.1	0.00077	100	126
Kosovo	619	0.00073	100	127
Israel	616.1	0.00073	100	128
New Zealand	585.9	0.00069	100	129
Denmark	517.2	0.00061	100	130
Germany	494	0.00058	100	131
Haiti	456	0.00054	100	132
Latvia	444.5	0.00052	100	133
Finland	420.5	0.0005	100	134
Lithuania	338	0.0004	100	135
Sweden	329	0.00039	100	136

Czech Republic	314.9	0.00037	100	137
Austria	311.1	0.00037	100	138
Slovakia	300.5	0.00035	100	139
Trinidad And Tobago	286.6	0.00034	100	140
Ireland	276.7	0.00033	100	141
Jamaica	273.6	0.00032	100	142
Libya	264.2	0.00031	100	143
French Guiana	224.2	0.00026	100	144
Estonia	176.4	0.00021	100	145
Norway	119.4	0.00014	100	146
Taiwan	102.8	0.00012	100	147
Jordan	95.05	0.00011	100	148
Palestine	81.18	0.0001	100	149
Lebanon	79.31	0.00009	100	150
Qatar	54.97	0.00006	100	151
Oman	52.34	0.00006	100	152
Brunei	44.8	0.00005	100	153
Belgium	41.37	0.00005	100	154
Slovenia	38.49	0.00005	100	155
Puerto Rico	24.46	0.00003	100	156
Switzerland	22.89	0.00003	100	157
Djibouti	19.2	0.00002	100	158
Iceland	15.32	0.00002	100	159
Yemen	13.08	0.00002	100	160
Netherlands	12.92	0.00002	100	161
United Arab Emirates	11.2	0.00001	100	162
Poland	8.749	0.00001	100	163
Equatorial Guinea	7.571	0.00001	100	164
Montserrat	4.315	0.00001	100	165
Barbados	3.505	0	100	166
Somaliland	3.348	0	100	167
Luxembourg	2.155	0	100	168
Saint Kitts And Nevis	0.8623	0	100	169
Cayman Islands	0.4321	0	100	170
British Virgin Islands	0.3291	0	100	171
Guadeloupe	0.2165	0	100	172

Table S2. South America. Mean values of each variable may be followed by trends that were significant according to a Thiel-Sen-Seigel regression.

Country	Peak Season (day of year)	Season Length (days)	Size (km^2)	Total Burned Area (Km^2)	Number of Fires	Maximum Single Day Growth (km^2)	Duration (days)	mean fire growth rate (km^2/day)
Argentina	200	106.2	1.7 (+)	835,400 (-)	482,500 (-)	0.9 (+)	3	0.4 (+)
Bolivia	239 (+)	38.4 (+)	3.9	754,600 (-)	191,500 (-)	1.5	4 (-)	0.5
Brazil	235	57.61 (+)	3 (+)	3818000	1,286,000 (-)	1.2 (+)	3.9 (+)	0.5 (+)
Chile	88	93.14	2.3	21,210 (+)	9,261 (+)	1.1	3.3	0.4
Colombia	92	113.6 (-)	2.9 (-)	446,700 (-)	153,800 (-)	1.3 (-)	3.7 (-)	0.5 (-)
Ecuador	289	54.65 (-)	1.1 (+)	4,768 (+)	4224	0.6 (+)	2.9 (+)	0.3
Guyana	186	123.2	1.5	16,420 (+)	11,120 (+)	1.4 (-)	3.7	0.7 (-)
Paraguay	203	82.8	1.5	495200	335600	0.8	3 (+)	0.3
Peru	239	49.3	0.9 (+)	20920	22040	0.5 (+)	2.9	0.3 (+)
Suriname	232	94.58	2.1	4736	2247	2.9	4.1 (-)	0.9
Uruguay	168	107.9	0.9	5,600 (-)	6,395 (-)	0.5	3	0.3
Venezuela	105	114	2.3	566300	247600	1	3.9	0.4

Note: Falkland Islands had insufficient fire activity for analysis.

Table S3. North America. Mean values of each variable may be followed by trends that were significant according to a Thiel-Sen-Seigel regression.

Country	Peak Season (day of year)	Season Length (days)	Size (km^2)	Total Burned Area (Km^2)	Number of Fires	Maximum Single Day Growth (km^2)	Duration (days)	mean fire growth rate (km^2/day)
Belize	108	27.98 (+)	1.2	7627	6,363 (+)	2.1 (-)	3.1	1.1 (-)
Canada	180	33.37	15 (+)	372900	24870	4.5	7.2	0.9
United States	181	80.06	2.4	666100	277,900 (-)	1.1 (+)	3.2	0.4
Costa Rica	108	100.2	1.6 (+)	7,071 (+)	4,333 (+)	1.5 (+)	4.4 (+)	0.7 (+)
Cuba	83	49.87 (+)	1.3 (-)	41,500 (-)	31,910 (-)	0.7 (-)	3.6 (-)	0.3 (-)
Dominican Republic	88 (+)	60.43 (+)	1.2 (-)	3,905 (-)	3,163 (-)	1.1 (-)	3.6 (+)	0.6 (-)
El_salvador	112	109.2 (-)	1.2 (+)	1,993 (+)	1,628 (+)	2.4 (+)	3.8	1.2 (+)
Guatemala	119 (+)	93.46 (+)	1.3	67450	50300	2	3.8 (+)	1.1 (-)
Haiti	110 (-)	126 (-)	1.2	456 (-)	388	1.9	3.5	1
Honduras	100	38.32	1.4	57630	42670	1.7	3.3	0.9
Jamaica	78 (+)	64.93 (+)	0.9 (+)	273.6	290	0.7 (+)	3.7	0.4 (+)
Mexico	125	54.56 (+)	1.6	328,100 (-)	203100	1	3.2 (-)	0.5
Nicaragua	108 (+)	76.31	1.4 (-)	38420	27100	1.6 (-)	3.6	0.8 (-)

Panama	79	26.93	1 (+)	7503	7640	0.6 (+)	3.2 (+)	0.3 (+)
The Bahamas	94	48.42	4.7	3408	731	1.6	5.7	0.5
Trinidad and Tobago	72	25.31	1 (+)	286.6	301	0.9 (+)	3.3	0.5

Note: United States Virgin Islands, Anguilla, Bermuda, Turks and Caicos Islands, Saint Vincent and The Grenadines, Saint Lucia, Aruba, Curaçao, Grenada, Saint Pierre and Miquelon, Saint Martin, Saint-Barthélemy, Dominica, Greenland, Antigua and Barbuda, and Sint Maarten had insufficient fire activity for analysis.

Table S4. Europe. Mean values of each variable may be followed by trends that were significant according to a Thiel-Sen-Seigel regression.

Country	Peak Season (day of year)	Season Length (days)	Size (km^2)	Total Burned Area (Km^2)	Number of Fires	Maximum Single Day Growth (km^2)	Duration (days)	mean fire growth rate (km^2/day)
Albania	222 (+)	22.45 (+)	2.8	2,706 (-)	965 (-)	5.4 (+)	4.3	2.1
Austria	182 (+)	56.68	1.3 (-)	311.1 (-)	239 (-)	1.2 (-)	2.6 (-)	0.6
Belarus	149	81.8	1.2 (+)	8825	7540	1.8 (+)	2.9	0.8 (+)
Bosnia and Herzegovina	187	74.32	2.9	4454	1547	6.3	3.8 (-)	2.5
Bulgaria	227 (+)	51.14 (-)	1.3	21,180 (-)	16,540 (-)	2.5	3.3 (+)	1.3
Croatia	185 (-)	74.21 (-)	1.9 (+)	2066	1,061 (-)	4.5	3.6	2 (+)
Czech Republic	193	65.31	0.6	314.9	543	0.7 (-)	2.4	0.5 (-)
Denmark	201 (+)	27.02	1.4 (-)	517.2 (-)	375 (-)	1.3 (-)	4	0.6 (-)
Estonia	139 (+)	57.2 (+)	0.9	176.4	190	1.5	2.6	0.7
Finland	111	36.75	1	420.5	421 (-)	0.9 (+)	2.4 (+)	0.5
France	173 (-)	74.54 (+)	1.3 (-)	7,218 (-)	5,639 (-)	0.9 (-)	3.1 (-)	0.5 (-)
Germany	181 (+)	65.87	1	494	488	1.1 (-)	3.1	0.6 (-)
Greece	232	48.99	3	12,280 (-)	4,119 (-)	1.6	3.6	0.6
Hungary	185 (-)	87.95	1.1	3,018 (-)	2,718 (-)	3.5	3.1 (-)	1.7 (-)
Ireland	113	23.09	1.5	276.7	189	1.5	3.4	0.7 (-)
Italy	224	40.73	1.9	19,120 (-)	10,230 (-)	1	3.3 (-)	0.5
Kosovo	219	56.49	2	619	313	7.4	4.2	3
Latvia	108 (+)	56.63	1.3	444.5 (-)	332 (-)	3.3	2.7 (-)	1.6
Lithuania	146 (+)	70.22 (-)	0.8 (-)	338 (-)	421 (-)	1.8 (-)	2.7	1 (-)
Moldova	205	55.99 (+)	0.9	6756	7740	1.6	3.1 (+)	0.9
Montenegro	214	45.83 (+)	2.5	1,535 (+)	617 (+)	6.3 (+)	4.4	2.6
Portugal	227	39.1	5.2	25660	4,959 (-)	5.4	3.9	1.6
Republic of Macedonia	221	55.91 (+)	2.3 (+)	1648	724	5.3 (+)	3.8	2.3
Romania	202	63.48	1.3	36,640 (-)	28,910 (-)	2.4	3.4	1.3
Russia	166	65.4	2.2 (+)	2,683,000 (-)	1,194,000 (-)	1 (+)	3 (-)	0.4 (+)
Serbia	252	50.16	1.4	8,234 (-)	5,903 (-)	4.1 (+)	3.2	2
Slovakia	183	63.91	0.9	300.5 (-)	328 (-)	2.2	3	1.2
Spain	211	67.73	2.7	21,020 (-)	7,785 (-)	2.6	3.6	1
Sweden	201	24.68	3.3	329	99	2.1	3.3 (+)	0.8
Ukraine	195	69.68 (+)	0.9 (+)	383800	409500	0.8 (+)	2.9	0.5 (+)
United Kingdom	113	42.7	1.4	795.6	571	1 (+)	3.1	0.5 (+)

Note: Vatican City, Jersey, Guernsey, Isle of Man, San Marino, Monaco, Malta, Liechtenstein, Åland Islands, Faroe Islands, and Andorra had insufficient fire activity for analysis.

Table S5. Asia and Oceania. Mean values of each variable may be followed by trends that were significant according to a Thiel-Sen-Seigel regression.

Country	Peak Season (day of year)	Season Length (days)	Size (km^2)	Total Burned Area (Km^2)	Number of Fires	Maximum Single Day Growth (km^2)	Duration (days)	mean fire growth rate (km^2/day)
Afghanistan	194	80.54	4.2 (-)	5,751 (-)	1,367 (-)	9.3	3.4	3.6
Armenia	260	72.12	1.8	2559	1458	1.2	3.4	0.5 (+)
Azerbaijan	206	39.97 (+)	3.5 (-)	36230	10350	1.6	3.5	0.6
Bangladesh	90	29.03 (+)	1.6	11,380 (-)	7287	0.8	3.2	0.4
Bhutan	91	64.16	2 (+)	1396	693	0.9 (+)	3.6 (+)	0.4 (+)
Cambodia	61 (+)	97.3	0.7 (-)	580,300 (-)	855400	0.5 (-)	1.3	0.4 (-)
China	149 (-)	81.16	2.2 (-)	664900	303100	1.2 (-)	2.7 (-)	0.5
East Timor	259	27.08 (-)	1.1	2,119 (-)	1,977 (-)	0.5	3.2	0.3 (-)
Georgia	192	74.4	2.5 (+)	4129	1,633 (-)	1.3 (+)	3.3	0.5 (+)
India	171 (+)	100.9	2.2 (+)	871,700 (+)	404,600 (+)	0.9 (+)	2.9	0.4 (+)
Indonesia	249	50.71	0.5 (+)	226600	427600	0.4 (+)	1.2 (+)	0.4 (+)
Iran	182 (-)	93.19	1.4 (-)	58,960 (-)	42330	1.5	3 (-)	0.8
Iraq	190	71.56 (-)	2	48,670 (+)	23,920 (+)	3 (-)	3	1.4 (-)
Israel	195	68.33	2 (-)	616.1 (-)	314	7.5	3.1	3.5
Japan	73	27.22	2.4 (-)	2670	1,100 (+)	1.4 (-)	3.5 (-)	0.5 (-)
Jordan	156	54.11 (+)	0.7	95.05	129 (+)	4.1 (-)	2.5 (-)	2.5 (-)
Kazakhstan	203	49.1	11.4	1,752,000 (-)	153,800 (-)	5.5	3.4 (-)	1.6
Kyrgyzstan	233	59.28 (+)	1.8 (-)	3,812 (-)	2,080 (-)	4.1 (-)	2.8 (-)	1.8 (-)
Laos	83 (+)	42.08 (-)	0.5 (-)	152200	326200	0.4 (-)	1.2 (-)	0.3 (-)
Malaysia	123	86.7 (-)	1.3	8,673 (-)	6,879 (-)	0.6	3.3	0.3
Mongolia	162	64.74 (+)	19.1	205,200 (-)	10,760 (-)	9.5	2.9	2.2
Myanmar	73 (+)	28.37 (+)	0.7 (-)	695,700 (-)	940,900 (-)	0.6 (-)	1.3	0.4 (-)
Nepal	98 (+)	31.4	4 (+)	38660	9561	1.5 (+)	4.1 (+)	0.6 (+)
North Korea	133	90.47 (-)	1.7 (-)	7,052 (-)	4240	1 (-)	2.9 (-)	0.4 (-)
Pakistan	158 (+)	91.82 (+)	1.2 (-)	39,090 (+)	33,640 (+)	1	2.8	0.4 (-)
Philippines	89 (-)	87.6 (-)	0.8 (+)	20770	27,390 (-)	0.4 (+)	2.8	0.3
Saudi Arabia	194 (+)	51.32 (+)	1.5 (-)	7,533 (-)	5,124 (-)	1.4 (-)	3 (-)	0.8 (-)
South Korea	74	40.53	2	656.1	332	1.4 (-)	3.1	0.6
Sri Lanka	201	41.43	1.5	7,554 (-)	5,169 (-)	0.7	3.4	0.3
Syria	197	54.81	1.8 (+)	16,820 (+)	9,164 (+)	2.8 (+)	3.1 (+)	1.2 (+)
Tajikistan	220 (-)	66.57	2.6 (-)	1,144 (-)	446 (-)	6.7 (-)	2.9	3.3 (-)
Thailand	83 (+)	82.24	0.5	308400	576900	0.4	1.2 (+)	0.4
Turkey	234 (+)	53.24 (+)	1.9 (-)	113200	59,250 (+)	0.9 (-)	3.1 (-)	0.4 (-)
Turkmenistan	171 (-)	77.53	3	29430	9975	3.7	3	1.4
Uzbekistan	142	82.97	2.3	11650	5163	4 (-)	3.3	1.7 (-)
Vietnam	86 (+)	74.8 (+)	0.6 (+)	194900	335700	0.5 (+)	1.3 (+)	0.4
Australia	238 (-)	85.07 (+)	7.7 (-)	9810000	1,280,000 (+)	2.7 (-)	2.1	1 (-)
New Zealand	157 (-)	124.6	1 (+)	585.9 (+)	572	0.6 (+)	2.6	0.3 (+)
Papua New Guinea	248	51.61	1.7 (-)	53390	31820	0.7 (-)	3.7	0.3 (-)

Note: Singapore, Kuwait, Turkish Republic of Northern Cyprus, Cyprus, Macau, Hong Kong, Bahrain, Australian Indian Ocean Territories and Siachen Glacier had insufficient fire activity for analysis.

Table S6. Africa. Mean values of each variable may be followed by trends that were significant according to a Thiel-Sen-Seigel regression.

Country	Peak Season (day of year)	Season Length (days)	Size (km^2)	Total Burned Area (Km^2)	Number of Fires	Maximum Single Day Growth (km^2)	Duration (days)	mean fire growth rate (km^2/day)
Algeria	218	27.94	3 (-)	19,640 (-)	6618	1.6 (-)	3.8 (-)	0.6
Angola	204	38.68 (+)	2.7 (-)	7,609,000 (-)	2,803,000 (+)	1.3 (-)	2.3	0.6 (-)
Benin	258 (-)	135.3 (+)	1.9	433,200 (-)	222,300 (-)	1.1 (-)	2	0.6
Botswana	248 (+)	52.2	22	1018000	46280	7.5 (-)	2.3 (+)	2.3
Burkina Faso	274	117.4	2.2	555,400 (-)	250,500 (-)	1.3	2.1	0.6
Burundi	195	35.45 (-)	1 (+)	8,122 (-)	8,467 (-)	0.7 (+)	1.9 (+)	0.4 (+)
Cameroon	247 (-)	139.5 (+)	1.4 (-)	838,200 (-)	586,500 (-)	0.8 (-)	1.9	0.5 (-)
Central African Republic	234 (-)	151.3 (+)	2.6 (-)	4,167,000 (-)	1597000	1.2 (-)	1.9 (+)	0.6 (-)
Chad	233 (-)	136.6	3.2 (-)	2,115,000 (-)	667,100 (-)	1.6 (-)	2.2 (-)	0.8 (-)
Democratic Republic of the Congo	179	63.3	1.6 (-)	7,050,000 (-)	4440000	0.9 (-)	2	0.5 (-)
Egypt	248 (-)	37.65 (+)	1.6	7768	4753	0.5 (+)	3.5 (-)	0.3 (+)
Eritrea	199 (-)	130.1	3.9 (-)	9,781 (-)	2512	3.2 (-)	2.6	1.3
Eswatini	220	39.76	1.1 (-)	16120	14410	0.8 (-)	2 (-)	0.5 (-)
Ethiopia	146 (-)	140.9	2.9 (-)	1,279,000 (-)	438200	1.5 (-)	2.2 (-)	0.7 (-)
Gabon	183 (+)	45.65 (-)	1.4 (+)	71420	51580	0.9 (+)	1.7	0.5 (+)
Gambia	109 (-)	105.4 (-)	4.1 (-)	49,040 (-)	12,010 (-)	2.7	4.3	0.9
Ghana	246	147.6	2.1	1,341,000 (-)	642,800 (-)	1.1	2 (+)	0.5
Guinea-Bissau	64 (+)	57.55 (+)	2.2 (-)	98,020 (-)	45,460 (-)	1.2 (-)	2.4	0.6 (-)
Guinea	147 (-)	143.7 (-)	1.1 (-)	871,000 (-)	759300	0.7 (-)	1.9	0.5 (-)
Ivory Coast	230 (+)	155.6 (-)	1.5 (+)	556,800 (-)	377,400 (-)	0.8	1.9	0.5
Kenya	144	109.2	1.3 (+)	67440	51,320 (-)	0.8 (+)	1.8 (+)	0.5 (+)
Lesotho	226 (+)	27.93 (+)	1.2 (-)	8,729 (-)	7,223 (-)	1	2.2	0.5
Liberia	88	34.08	0.6 (-)	16360	29420	0.4 (-)	1.4	0.3 (-)
Libya	230 (-)	85.03 (+)	1.8	264.2 (+)	150 (+)	1	3.5	0.5
Madagascar	233 (-)	59.41 (+)	1.6 (-)	859,500 (-)	526400	0.8 (-)	3.2 (-)	0.4 (-)
Malawi	246	44.41 (+)	0.9	111,100 (-)	129,200 (-)	0.6 (-)	1.4	0.5 (-)
Mali	238 (-)	119.5	3.9 (-)	1,480,000 (-)	379,800 (-)	1.8 (-)	3.6 (-)	0.7 (-)
Mauritania	217	120.4	18.4 (-)	58,090 (-)	3,161 (-)	11.8 (-)	3.5	3.9 (-)
Morocco	218	48	2	1037	521	1.1	3.5	0.5
Mozambique	244	35.02 (-)	1.9 (-)	4,058,000 (-)	2143000	0.9 (-)	2.1	0.5 (-)
Namibia	244	40.82 (+)	12.4 (-)	778,400 (-)	62650	5 (-)	2.7	1.7 (-)
Niger	254	111.7	5.3 (-)	57,880 (+)	10,890 (+)	3.8 (-)	2.5	1.5 (-)
Nigeria	159 (+)	157.7 (-)	1.7	1,783,000 (-)	1,037,000 (-)	0.9	2	0.5 (-)
Republic of the Congo	173	61.61	1 (+)	687200	671600	0.7	1.6	0.5
Rwanda	190	59.02	1.6	7,616 (+)	4,863 (+)	1.1	1.8	0.6
Senegal	214 (-)	132.7 (+)	6.1	922,000 (-)	150,800 (-)	2.5 (-)	4.1 (-)	0.8 (-)
Sierra Leone	96	110.2	1 (-)	180000	189400	0.6 (-)	1.7	0.4 (-)
Somalia	130	104 (-)	0.9	5,232 (-)	5,779 (-)	0.6	1.8	0.4 (+)
South Africa	222	61.97 (+)	2.2 (-)	782,500 (-)	356,800 (-)	1.3 (-)	2.1	0.7
South Sudan	238	141.6	4.5 (-)	6352000	1,397,000 (+)	1.9 (-)	2.1	0.8 (-)
Sudan	248	115.5 (+)	3.3 (-)	1,600,000 (-)	480,000 (-)	1.9 (-)	2.2 (-)	0.8 (-)
Tanzania	212 (+)	47.37	1.7 (+)	2,700,000 (-)	1,562,000 (-)	0.9	1.9 (-)	0.5 (+)
Togo	248 (-)	148.6 (+)	1.4	230,500 (-)	165,900 (-)	0.9	1.9	0.5
Tunisia	222 (-)	32.55	2.5 (+)	1,587 (+)	635 (+)	1.5 (+)	3.6 (+)	0.6 (+)
Uganda	193 (-)	153.7	1.8 (-)	596,300 (-)	336100	1 (-)	2	0.5 (-)
Zambia	221	37.61	2.5 (-)	4,754,000 (-)	1905000	1.2 (-)	2.4	0.6 (-)
Zimbabwe	248 (+)	35.98 (+)	2.9 (-)	652,000 (-)	228,300 (-)	1.6 (-)	2.4	0.8 (-)

Note: São Tomé and Príncipe, Western Sahara, Comoros and Cape Verde had insufficient fire activity for analysis.

Table S7. Fit metrics for linear mixed models from figure 5. Conditional R^2 is the variance explained by the whole model, while marginal R^2 is the variance explained by the fixed effects.

Climate Region	Fire Regime Component	Conditional R^2	Marginal R^2	% Explained by Random Effects
Boreal	Duration	0.625	0.003	62.2
Boreal	Max Growth	0.689	0.046	64.3
Boreal	Mean Growth	0.763	0.091	67.2
Boreal	Size	0.514	0.129	38.6
Arid	Duration	0.603	0.012	59.1
Arid	Max Growth	0.75	0.134	61.5
Arid	Mean Growth	0.798	0.126	67.2
Arid	Size	0.739	0.215	52.4